Earth Syst. Sci. Data, 17, 4125–4157, 2025
https://doi.org/10.5194/essd-17-4125-2025

Open Access Earth System Science Data

Rock Glacier Inventories (RoGIs) in 12 areas worldwide using a multi-operator consensus-based procedure

Line Rouyet[1,2], Tobias Bolch[3,4], Francesco Brardinoni[5], Rafael Caduff[6], Diego Cusicanqui[7], Margaret Darrow[8], Reynald Delaloye[1], Thomas Echelard[1,5], Christophe Lambiel[9], Cécile Pellet[1], Lucas Ruiz[10], Lea Schmid[1], Flavius Sirbu[11], and Tazio Strozzi[6]

[1]Department of Geosciences, University of Fribourg (UNIFR), 1700 Fribourg, Switzerland
[2]NORCE Norwegian Research Centre AS, 9294 Tromsø, Norway
[3]Institute of Geodesy, Graz University of Technology (TU Graz), 8010 Graz, Austria
[4]Central-Asian Regional Glaciological Centre of Category 2 under the auspices of UNESCO, 050010 Almaty, Kazakhstan
[5]Department of Biological, Geological, and Environmental Sciences, University of Bologna (UniBo), 40126 Bologna, Italy
[6]GAMMA Remote Sensing AG, 3076 Gümligen, Switzerland
[7]Institut des Sciences de la Terre (ISTerre), Université Grenoble Alpes (UGA), 38400 Saint-Martin-d'Hères, France
[8]Department of Civil, Geological, and Environmental Engineering, University of Alaska Fairbanks (UAF), Fairbanks, AK 99775-5900, United Stated of America
[9]Institute of Earth Surface Dynamics, University of Lausanne (UNIL), 1015 Lausanne, Switzerland
[10]Argentine Institute of Nivology, Glaciology and Environmental Sciences (IANIGLA), 5500 Mendoza, Argentina
[11]Institute of Advanced Environmental Research, West University of Timişoara (WUT), 300223 Timişoara, Romania

Correspondence: Line Rouyet (line.rouyet@unifr.ch, liro@norceresearch.no)

Received: 16 December 2024 – Discussion started: 14 January 2025
Revised: 20 May 2025 – Accepted: 3 June 2025 – Published: 27 August 2025

Abstract. The Rock Glacier Inventories and Kinematics (RGIK) community has defined standards for generating Rock Glacier Inventories (RoGIs). In the framework of the European Space Agency Climate Change Initiative for Permafrost (ESA CCI Permafrost), we set up a multi-operator mapping exercise in 12 areas around the world. Each RoGI team was composed of 5 to 10 operators, involving 41 persons in total. Each operator performed similar steps following the RGIK guidelines (RGIK, 2023a) and using a similar QGIS tool. The individual results were compared and combined after common meetings to agree on the final consensus-based solutions. In total, 337 "certain" rock glaciers have been identified and characterised, and 222 additional landforms have been identified as "uncertain" rock glaciers.

The dataset consists of three GeoPackage (gpkg) files for each area: (1) the primary markers (PMs) locating and characterising the identified rock glacier units (RGUs), (2) the moving areas (MAs) delineating areas with surface movement associated with the rock glacier creep based on spaceborne Interferometric Synthetic Aperture Radar (InSAR), and (3) the geomorphological outlines (GOs) delineating the restricted and extended rock glacier unit (RGU) boundaries. Here we present the procedure for generating consensus-based RoGIs, describe the data properties, highlight their value and limitations, and discuss potential applications. The final PM/MA/GO dataset is available on Zenodo (Rouyet et al., 2025; https://doi.org/10.5281/zenodo.14501398). The GeoPackage (gpkg) templates for performing similar RoGIs in other areas and exercises based on the QGIS tool are available on the RGIK website (https://www.rgik.org, last access: 15 August 2025).

Published by Copernicus Publications.

1 Introduction

Permafrost is defined as subsurface material remaining at or below 0 °C for at least 2 consecutive years (French, 2007). Due to its sensitivity to climate change, permafrost is an essential climate variable (ECV), traditionally documented by the ground temperature (GT) and the active layer thickness (ALT) (Streletskiy et al., 2017). In mountains, the permafrost distribution may be discontinuous and controlled by site-specific conditions with large variations over short distances. The investigation of mountain permafrost requires the development of dedicated products to complement to GT and ALT measurements and models. Rock glaciers are obvious expressions of mountain permafrost defined as debris landforms generated by the former or current creep of frozen ground (RGIK, 2023a). Although contrasting views exist in the genetic origin of rock glaciers, the distribution of rock glaciers may be regarded as a proxy for past or present permafrost occurrences. Rock Glacier Inventories (RoGIs), including relict, transitional, and active landforms, are valuable to understand the evolution of periglacial environments and to calibrate or validate mountain permafrost distribution models where in situ measurements are scarce (Azócar et al., 2017; Boeckli et al., 2012; Etzelmüller et al., 2020; Karjalainen et al., 2020; Marcer et al., 2017; Schmid et al., 2015). The distribution, sizes, and dynamics of rock glaciers also have several operational implications for the management of geohazards and water resources, which have justified RoGI compilation in many mountain ranges (Hassan et al., 2021; Jones et al., 2018; Marcer et al., 2019; Rangecroft et al., 2015).

In addition, rock glacier creep rate is influenced by the permafrost thermal state and the ground ice/water contents (Cicoira et al., 2019; Ikeda et al., 2008; Kenner et al., 2020). Several studies demonstrated that the interannual rock glacier velocity (RGV) changes relate to the ground temperature variations (Delaloye et al., 2008, 2010; Kääb et al., 2007; Kellerer-Pirklbauer et al., 2024; Schoeneich et al., 2015; Staub et al., 2016). In the context of climate change, cases of acceleration, destabilisation, and even collapse have been reported (Bodin et al., 2017; Delaloye et al., 2013; Eriksen et al., 2018; Hartl et al., 2023; Kellerer-Pirklbauer et al., 2024; Scotti et al., 2017). Conversely, as degradation continues, rock glaciers tend to decelerate and transition progressively into relict landforms (Ikeda and Matsuoka, 2002; Manchado et al., 2024; Necsoiu et al., 2016). Due to the link between temperature and rock glacier creep rate, rock glacier velocity (RGV) became a new product of the ECV Permafrost (Hu et al., 2025; Streletskiy et al., 2021; WMO, 2022). In this context, RoGI compilation can be considered a first necessary step to identify and select landforms to be monitored in a climate-oriented perspective. However, RoGIs are not exhaustive worldwide, and existing RoGIs have been compiled with various methodologies. Owing to a lack of concerted international rules for mapping and characterising rock glaciers, a RoGI compiled by different operators may lead to high levels of variability (Brardinoni et al., 2019), which hampers our ability to compare, merge, and analyse inventories across different regions.

With these motivations, the Rock Glacier Inventories and Kinematics (RGIK) initiative, launched in 2018, has focused on defining widely accepted standards and developing guidelines for the generation of RoGI and RGV products (Delaloye et al., 2018). With the long-term objective to generate a homogeneous open-access RoGI database, RGIK has released RoGI guidelines defining rules for inventory rock glaciers (RGIK, 2023a). In parallel, the European Space Agency Climate Change Initiative for Permafrost (ESA CCI Permafrost) has worked on scaling up the generation and evaluation of ECV permafrost products using satellite remote sensing (Bartsch et al., 2023; Trofaier et al., 2017). For rock glacier products, ESA CCI Permafrost especially focuses on the use of spaceborne Interferometric Synthetic Aperture Radar (InSAR), an established remote sensing technique documenting ground surface movement and widely applied in the RoGI framework (Bertone et al., 2024; Brencher et al., 2021; Hu et al., 2023; Lambiel et al., 2023; Liu et al., 2013; Ma and Oguchi, 2024; Reinosch et al., 2021; Rouyet et al., 2021).

Previous studies highlighted the inherent subjectivity of operators to interpret the morpho-kinematic characteristics of rock glaciers based on optical and InSAR data (Bertone et al., 2022) and the benefits of designing multi-operator consensus-based procedures to reduce discrepancies and improve the final products (Way et al., 2021). In 2023, we therefore designed a mapping exercise with teams including operators from diverse institutions, countries, and backgrounds. This multi-operator RoGI exercise was performed in 12 areas around the world. Several operators performed similar steps individually and then discussed the results to provide consensus-based final products. This unique international initiative had four main objectives: (1) train the community for RoGI production, (2) test common RoGI rules and identify discrepancies to refine the existing guidelines, (3) develop standardised GIS templates and training tools for enhancing the production of comparable RoGIs in new regions, and (4) compile and disseminate a homogenised set of RoGIs from 12 diverse regions.

Here we present the multi-operator inventorying procedure (Sect. 2), describe the GIS tool and data properties (Sect. 3), summarise the main characteristics of the resulting dataset (Sect. 4), discuss the uncertainties and limitations (Sect. 5), and suggest ideas for future use and applications (Sect. 6).

2 Multi-operator inventorying procedure

2.1 RoGI areas and teams

The exercise was performed in 12 areas selected in 10 countries and 5 continents (Table 1; Fig. 1). Most RoGI areas have been selected within larger regions previously studied by Bertone et al. (2022), who included detailed descriptions of the regional settings in the article supplement. A principal investigator (PI) was designated to coordinate the work of the inventory team in each area. All PIs had past or ongoing research in the area they were leading. The volunteer operators were found within the involved institutions and after a call for participation in June 2023 using the RGIK mailing list (about 200 subscribers). The participants were free to choose one or more area(s) to perform the work depending on their interest and time availability. To ensure there were enough operators in each area, as well as a diversity of geographical background, competence, and seniority, members of the PI team acted as operators in areas where few people signed up. The resulting inventory teams were composed of 5 to 10 operators (including the PI; Table 1). Some operators worked in several areas. One operator (R. Delaloye) performed the work in all the areas, which helped communicating common challenges and coordinating key decisions across the teams. The exercise involved a total of 41 persons (see author list and acknowledgements).

2.2 Consensus-based RoGI procedure

The RoGI exercise was performed between June and November 2023. The University of Fribourg (UNIFR), Switzerland, was responsible for providing the data packages and instructions and coordinating the work between the 12 teams, corresponding to the 12 areas. For each area, the PI coordinated the work and was responsible for the final products. The PI also performed the work as an operator. Within each team, each operator received a common folder including a similar dataset applicable for the area. The data were organised within a QGIS project (see Sect. 3.1), along with the instructions for the exercise and the references to the RGIK guidelines applicable at the time (RGIK, 2022a, b, c, 2023b). The guidelines have since been merged into one reference document (RGIK, 2023a).

The inventory procedure included two main phases, performed in June–September 2023 (Phase 1) and in September–November 2023 (Phase 2) (Fig. 2). Each phase was divided into three steps:

- *Step A:* individual work by each team operator. At the end of this step, all the operators sent their results to the PI.
- *Step B:* compilation and summary by the PI. When discrepancies between operators were identified, the PI suggested a solution to be discussed with the team.
- *Step C:* discussion and consensus-based final decision by the inventory team. At the end of this step, the team agreed to the intermediate (first phase) or the final outputs (second phase).

During the first phase performed between June and September 2023, the team had to

- identify and locate the rock glacier units (RGUs) with primary markers (PMs). The operators were asked to include landforms following the technical definition of a rock glacier: "a debris landforms generated by the former or current creep of frozen ground, detectable in the landscape with the following morphologies: front, lateral margins and optionally ridge-and-furrow surface topography" (RGIK, 2023a, p. 6). Based on this definition, a RoGI must include relict rock glaciers but discard landforms that are primarily driven by other processes, such as glacial flow, solifluction, ice melt, and sliding along a slip surface. Different units are discriminated according to the RGIK guidelines (RGIK, 2023a). Orthoimages were the primary source of data used for this task, but additional datasets were used when available (e.g. digital elevation model, DEM) (see Sect. 3.1). InSAR data were useful to detect or confirm the location of moving rock glaciers. Each recognised RGU was identified with a point (primary marker, PM) in a dedicated vector layer. An uncertainty could be expressed by defining the landform as "uncertain" rock glacier in the case of geomorphological ambiguity or low data quality. When combining the results between operators, the team agreed on which units were categorised as "certain" or "uncertain" within each area. In some cases, the rock glaciers remained "uncertain" when there was not enough evidence that the landform is a rock glacier or when the teams decided that the landform was too complex to be accurately characterised and outlined with the currently available data. Keeping an information about the location of these uncertain landforms may allow for future updates if new data are becoming available. The operators could optionally use a label "not a rock glacier" to indicate landforms that may be mistaken for rock glaciers but are not driven by permafrost creep. These complex cases were discussed during team meetings and sometimes kept in the final layer for educational purposes. The attribute table of the PM layer is shown in Appendix A. At this stage, only the first attributes of the table were applicable as the detailed morpho-kinematic characterisation was performed during the second stage.
- detect, delineate, and classify moving areas (MAs) using InSAR. This task was performed in parallel, potentially iteratively, with the first bullet point (RGU identification with PM). The MAs were identified, delineated, and characterised based on InSAR data (see Sect. 3.1).

Table 1. RoGI areas and teams (PI acronyms: see author list and affiliations).

Area number (ESA CCI Permafrost convention)	Area name *(country, code)* Approx. central lat and long location	AOI km^2 Elevation range	PI (institution) *(# of operators, incl. the PI)*
Area 5-1	Carpathians *(Romania, RO)* 45°23′ N, 22°53′ E	18 ∼ 1070 to ∼ 2500 m a.s.l.	FS / WUT *(7 operators)*
Area 6-1	Western Alps *(Switzerland, CH)* 46°11′ N, 7°30′ E	12 ∼ 2160 to ∼ 3000 m a.s.l.	TE / UNIFR *(5 operators)*
Area 7-1	Troms *(Norway, NO-T)* 69°23′ N, 20°26′ E	47 ∼ 400 to ∼ 1400 m a.s.l.	LRo / NORCE *(6 operators)*
Area 8-1	Finnmark *(Norway, NO-F)* 70°45′ N, 27°50′ E	15 0 to ∼ 535 m a.s.l.	LRo / NORCE *(7 operators)*
Area 9-1	Nordenskiöld Land *(Norway, NO-N)* 77°53′ N, 13°54′ E	10 ∼ 50 to ∼ 900 m a.s.l.	LRo / NORCE *(6 operators)*
Area 10-1	Vanoise Massif *(France, FR)* 45°19′ N, 6°37′ E	37 ∼ 1710 to ∼ 3150 m a.s.l.	DC / USMB/UGA *(6 operators)*
Area 11-1	Southern Venosta *(Italy, IT)* 46°33′ N, 10°36′ E	19 ∼ 2120 to ∼ 3545 m a.s.l.	FB / UniBo *(10 operators)*
Area 12-1	Disko Island *(Greenland, GL)* 69°51′ N, 52°33′ W	82 0 to ∼ 1330 m a.s.l.	RC / GAMMA *(6 operators)*
Area 13-1	Northern Tien Shan *(Kazakhstan, KA)* 43°0′ N, 77°1′ W	59 ∼ 2570 to ∼ 4365 m a.s.l.	TB / TU Graz *(7 operators)*
Area 14-1	Brooks Range *(Alaska, US)* 68°6′ N, 149°58′ W	21 ∼ 1120 to ∼ 2070 m a.s.l.	MD / UAF *(10 operators)*
Area 15-1	Central Andes *(Argentina, AR)* 32°59′ S, 69.34° W	55 ∼ 3570 to ∼ 5530 m a.s.l.	LRu / IANIGLA *(10 operators)*
Area 16-1	Southern Alps *(Aotearoa New Zealand, NZ)* 43°59′ S, 170°3′ E	7 ∼ 1600 to ∼ 2431 m a.s.l.	CL / UNIL *(7 operators)*

For each area, the operators used a similar collection of radar image pairs (interferograms) from different spaceborne radar sensors, with different viewing geometries and variable time intervals between the image acquisitions. In some areas, multi-temporal InSAR mean velocity maps based on distributed scatterer (DS) and persistent scatterer (PS) algorithms were also available (Table 2). Each recognised MA was delineated in a dedicated polygon vector layer. The attributes documenting the velocity class, the observation time window and validity time frame, and the MA reliability could be filled using a semi-automatic dialog box. The attribute table of the MA layer is shown in Appendix B. The boundaries of the MA polygons follow the InSAR signal, not the landform features. If the movement is heterogeneous and/or if InSAR is affected by limitations, the MAs may only be partly overlapping with the rock glacier. The MA step was performed before the team decisions on the RGU final locations, which means that some delineated MA may correspond to surface movement associated with uncertain rock glaciers or other periglacial processes. Such polygons were kept in the final layer but were not further used for morpho-kinematic characterisation when they did not correspond to a certain RGU. If no movement was detected on InSAR, no polygon was drawn. Several rock glaciers have therefore no corresponding MA. The complete procedure is explained in the RGIK practical InSAR guidelines (RGIK, 2023b).

In September 2023, the PI compared the individual results and suggested final solutions. After a discussion and adjustment during an online meeting with the team operators, the final consensus-based PM and MA layers were adopted.

During the second phase performed between September and November 2023, the team focused on the landforms categorised as "certain" rock glaciers in the final PM layer. For those landforms, the operators had to

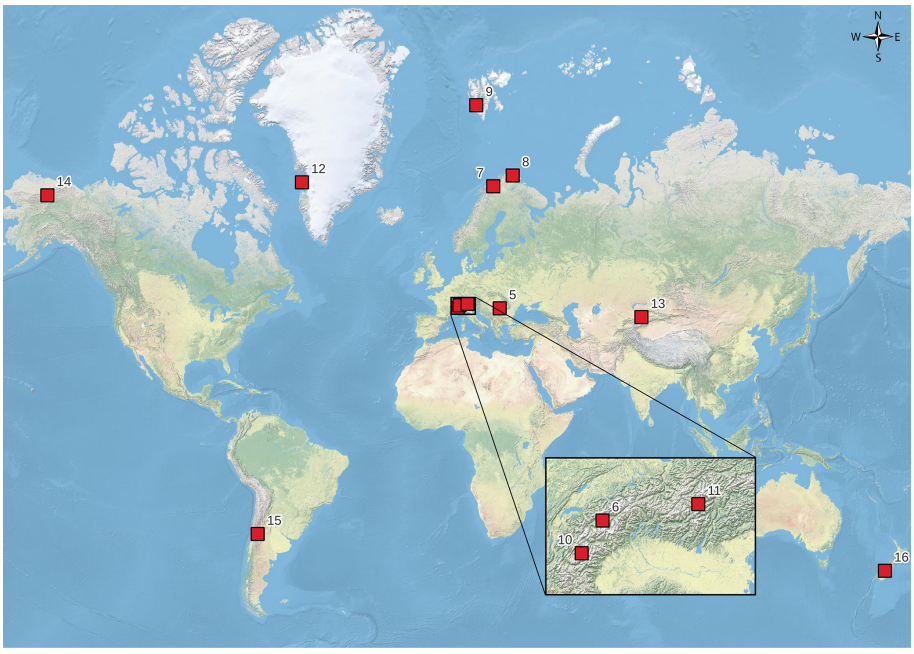

Figure 1. Location map of the RoGI regions, including the areas selected for the multi-operator RoGI exercise. Background map: ESRI Physical Web Map Service.

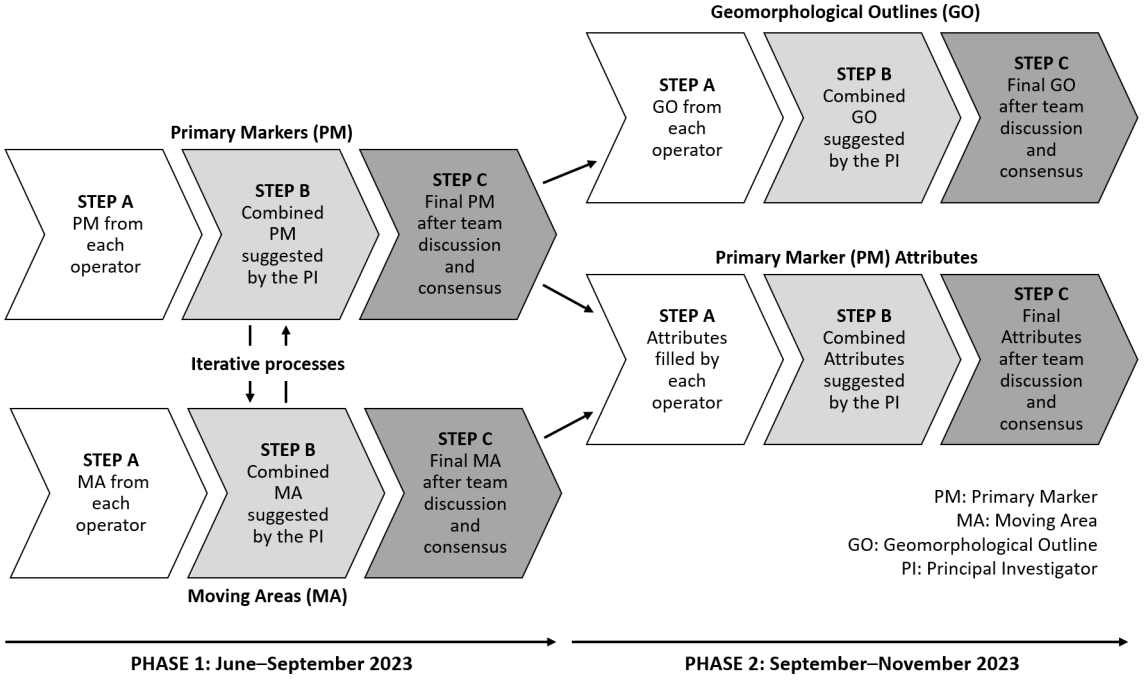

Figure 2. Consensus-based RoGI procedure.

– document the RGU morpho-kinematic characteristics (attributes). The morpho-kinematic attributes characterising the RGUs were filled using a semi-automatic dialog box in the final consensus-based PM layer from the first phase. All attributes refer to definitions described in the RGIK RoGI guidelines (RGIK, 2023a). All documented attributes are listed in Appendix A. For the geomorphologic attributes, orthoimages were the primary source of data, but additional datasets were used (e.g. DEM) (see Sect. 3.1, Table 2). The kinematic attribute (KA) is a semi-quantitative estimate of the overall multi-annual movement rate of the rock glacier unit

Table 2. Summary of input data in each RoGI area. The names and locations corresponding to the area numbers are shown in Table 1. The crosses (x) highlight the availability of the corresponding dataset. For InSAR data: the yy–yy numbers correspond to the years available for each InSAR dataset (e.g. 15–19: interferograms or averaged velocity maps between 2015 and 2019).

Area number (see Table 1)	5-1	6-1	7-1	8-1	9-1	10-1	11-1	12-1	13-1	14-1	15-1	16-1
Satellite Web Map Services (WMS): optical imagery and topographical map												
Google satellite WMS	x	x	x	x	x	x	x	x	x	x	x	x
Bing satellite WMS	x	x	x	x	x	x	x	x	x	x	x	x
ESRI satellite WMS	x	x	x	x	x	x	x	x	x	x	x	x
OpenTopoMap WMS	x	x	x	x	x	x	x	x	x	x	x	x
Additional optical/thematic data: HR aerial imagery and national topographical map												
Extra HR aerial image	x	x	x	x	x	x						
National topo. map		x	x	x		x						x
DEM products: low-/high-resolution (LR/HR) DEM and/or associated products (e.g. hill shades, slope, and aspect)												
LR DEM (10–30 m)	x	x	x	x	x	x	x	x	x	x	x	x
HR DEM (< 10 m)	x	x				x	x					
InSAR data: wrapped interferograms (ifgs) and velocity maps from stacking and persistent scatterer interferometry (PSI)												
Sentinel-1 ifgs	16–19	17–19	17–19	17–20	18–20	16–19	18–19	15–19	15–19	16–19	18–20	15–23
ERS-1/2 ifgs									98–99	91–95		
ALOS-1 ifgs						07–10	07–10		06–10	06–09	08–11	07–08
ALOS-2 ifgs	14–19	14–21						15–17	14–16	15–16	16–19	
SAOCOM ifgs		21									21–22	21–23
Cosmo-SkyMed ifgs							16–20					
TerraSAR-X ifgs		09–14										
6–12 d ifgs stacking		19	15–19	15–20	15–20	18–19	18–19	18	18	18–19	18–19	18
Combined 6 d–annual ifgs stacking			15–19	15–20	15–20							
PSI	15–21			15–19								

(order of magnitude: $\mathrm{cm\,yr^{-1}}$, $\mathrm{dm\,yr^{-1}}$, $\mathrm{m\,yr^{-1}}$, etc.), summarising the information provided by the MA layer when it overlaps with the identified rock glacier landforms. The procedure to convert velocity information from one or several MA polygons to one KA category is explained in the RGIK guidelines (RGIK, 2023a, b). The KA was used to assess the activity (active, transitional, relict) defined as the efficiency of sediment conveyance (expressed by the surface movement).

– delineate the RGU geomorphological outlines (GOs). The extended and restricted rock glacier GOs were delineated in a dedicated polygon vector layer. The extended outline embeds the entire rock glacier up to the rooting zone and includes the external parts (front and lateral margins). The restricted outline embeds the entire rock glacier up to the rooting zone excluding the external parts (front and lateral margins) (RGIK, 2023a). For each polygon, attributes (outline type and reliability of the delineation) could be filled using a semi-automatic dialog box. The attribute table of the GO layer is shown in Appendix C.

In November 2023, the PI compared the individual results and suggested final solutions. After a discussion and adjustment during an online meeting with the team operators, the final consensus-based PM attributes and the GO layer were adopted.

The compilation, data harmonisation, and technical correction of the final set of PM, MA, and GO products were performed by the University of Fribourg, Switzerland (UNIFR), between November 2023 and February 2024. A final verification and approval by the PIs were performed between February and May 2024. Thanks to the referee's comments on the first submission of the dataset and the associated paper, new corrections were inserted in March 2025.

3 Data types, attributes, and formats

3.1 Input data and GIS tool

The data packages delivered to the operators all had the same structure. The content was similar for each area. The main folder included four subfolders and a QGIS project:

– subfolder "INSTRUCTIONS" with the documents and links to the applicable guidelines.

- subfolder "VECTOR" including the polygon of the area of interest (AOI) that defined the boundaries in which the inventory work had to be performed as well as the initial GeoPackage (gpkg) templates for digitalising the PM, MA, and GO.
- subfolder "INSAR-DATA" including wrapped interferograms from Sentinel-1 (and potentially ALOS, SAOCOM, Cosmo-SkyMed, and/or TerraSAR-X depending on the data availability), potential complementary InSAR products (e.g. velocity maps from 6–12 d stacking, combined 6 d–annual stacking, and/or persistent scatterer interferometry algorithms), a layer displaying an index to reproject the line-of-sight displacement rate along the direction of the steepest slope (normalisation factor), or a mask highlighting north–south-facing slopes where the InSAR data are likely to underestimate the real movement. These datasets are summarised in Table 2 and further explained in the InSAR guidelines (RGIK, 2023b).
- subfolder "DEM-ORTHO" in which the PI could add extra available background data before delivery to the operators (e.g. DEM-based products, high-resolution orthophotos, and topographic maps; see Table 2).
- QGIS project structuring the available data and in which the operators performed the work. In addition to the AOI, the InSAR data and initial vector files (gpkg templates), each GIS project incorporated links to Web Map Services (WMS) such as the Google Earth, Bing and ESRI orthomosaics (Table 2). The spatial resolution of such images is typically 0.1–1 m but varies within/across the areas and depending on the scale and zoom levels.

The work was performed in similar QGIS projects, with a common file structure, background data, and dialog boxes for filling the attribute tables. The QGIS structure is generic and allows for semi-automatic attribute selection to simplify the work of the operators (Fig. 3).

3.2 Output data: format and properties

The RoGI multi-operator exercise led to the generation of a set of three files for each area: the RGU primary markers (PMs), the InSAR-based moving areas (MAs), and the RGU geomorphological outlines (GOs). All datasets are provided in a GeoPackage vector format (gpkg), a platform-independent database container. The coordinate reference system (CRS) used for the RoGI products is the World Geodetic System 1984 (WGS84). The coordinates are specified in decimal degrees.

For the RGU primary markers (PMs), the following attributes are documented:

- ID (unique alpha-numerical identifier of the RGU).
- X and Y coordinates (WGS84 coordinate system).
- Morphological type (simple, complex).

  Additional related attribute: the "Completeness" field defining if the rock glacier is completely visible or not (complete, unclear connection to the upslope, truncated front, uncertain).
- Spatial connection to the upslope unit (talus-, debris mantle-, landslide-, glacier-, glacier forefield-, and polyconnected; other; uncertain; and unknown).

  Additional related attributes are the "Upslope current" field defining if the rock glacier is currently connected to the upslope unit or not, and a "Comment" field to further describe morphological characteristics.
- Kinematic attribute ($< \mathrm{cm\,yr^{-1}}$, $\mathrm{cm\,yr^{-1}}$, $\mathrm{cm\,yr^{-1}}$ to $\mathrm{dm\,yr^{-1}}$, $\mathrm{dm\,yr^{-1}}$, $\mathrm{dm\,yr^{-1}}$ to $\mathrm{m\,yr^{-1}}$, $\mathrm{m\,yr^{-1}}$, $> \mathrm{m\,yr^{-1}}$, undefined).

  Additional related attributes are the "Type of Data" field to define the type of data used to assign the kinematic attribute (optical, radar, lidar, geodetic, other), the "Kinematic period" field to document the applicable period of the kinematic attribute (year(s) with available data), the "Reliability" of the kinematic attribute (low, medium, high, undefined), and a "Comment" field to document the applied method and the data quality.
- Activity (active, active uncertain, transitional, transitional uncertain, relict, relict uncertain, uncertain).

  Additional related attribute are the "Activity assessment" field documenting how the activity has been assessed (morphological evidence only or with kinematic data).
- Destabilisation signs (yes – ongoing, yes – completed, no, undefined).

For the moving areas (MAs), the following attributes are documented:

- ID (unique alpha-numerical identifier of the moving area),
- velocity class ($< 1\,\mathrm{cm\,yr^{-1}}$, $1–3\,\mathrm{cm\,yr^{-1}}$, $3–10\,\mathrm{cm\,yr^{-1}}$, $10–30\,\mathrm{cm\,yr^{-1}}$, $30–100\,\mathrm{m\,yr^{-1}}$, $> 100\,\mathrm{cm\,yr^{-1}}$),
- time observation window (text documenting the time period used for the MA detection and characterisation),
- reliability of the detected moving area (low, medium, high),
- additional comments.

For the geomorphological outlines (GOs), the following attributes are documented:

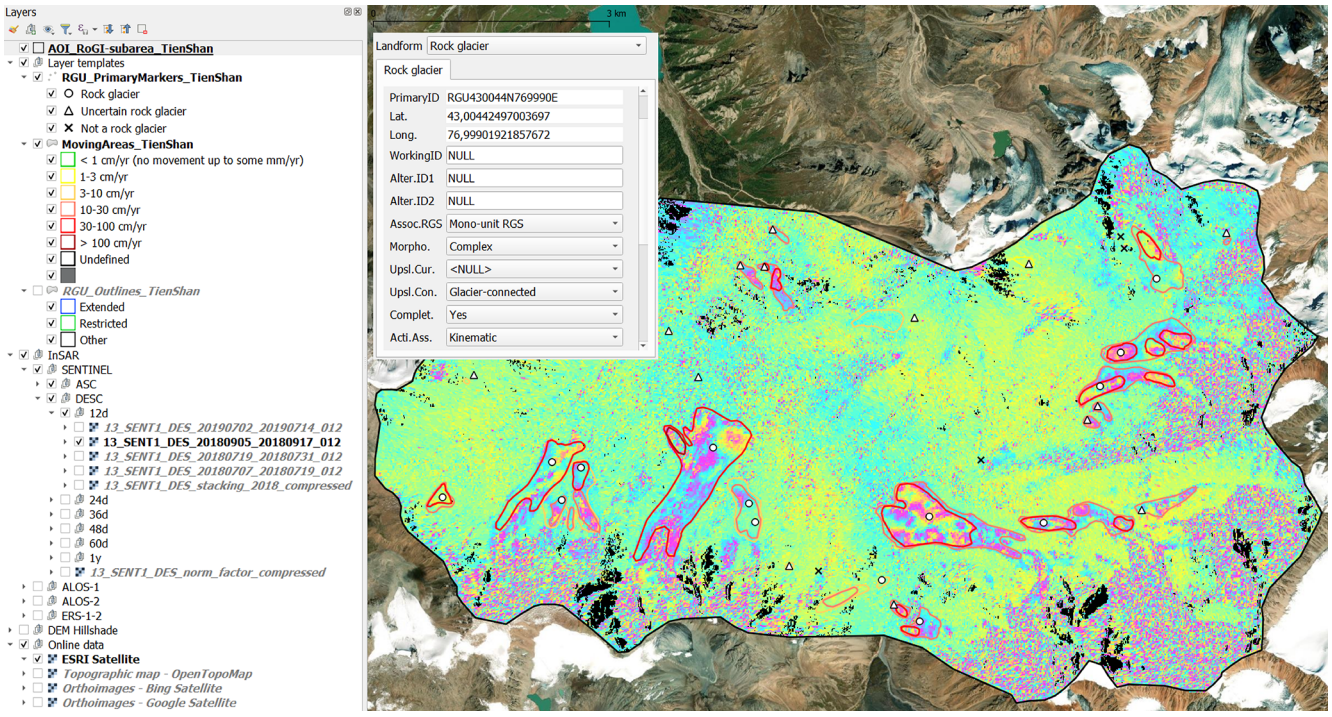

Figure 3. Example of QGIS data structure and dialog box for semi-automatic attribute filling in area 13-1 (northern Tien Shan, Kazakhstan). An example of a Sentinel-1 wrapped interferogram is displayed within the AOI extent. The boundaries of the RoGI area (black polygon), the PM (white dots and triangles), and the MA (yellow to red polygons) are displayed as top layers. For the sake of visualisation, the GO layer is not shown. See the example with GO in Fig. 4. Background map: ESRI Satellite Web Map Service.

- ID (unique alpha-numerical identifier of the moving area);
- outline type (extended, restricted, other);
- reliability of the front, left margin, right margin, and upslope limit (0 – low, 1 – medium, 2 – high) and reliability index (automatic summation of the values assigned to the reliability attributes of these four different boundaries);
- additional comments.

Each attribute is explained in detail in Appendixes A–C (including references to the applicable sections of the RGIK guidelines).

3.3 Output data: structure and naming convention

The data package is available on Zenodo (Rouyet et al., 2025; https://doi.org/10.5281/zenodo.14501398). It includes a set of gpkg files organised by areas and product types (PM, MA, GO).

The naming convention of each gpkg file follows the product specifications defined by the ESA CCI Permafrost project and is meant to provide a generic structure allowing for updates and/or the release of future additional products. All file names follow the same structure: ESACCI-<CCI Project>-<Processing Level>_<Data Type>_<Product String>-<Additional Segregator>_<Layer Type>_<Indicative Date>-fv<File version>.gpkg

- <*CCI Project*>: PERMAFROST.
- <*Processing Level*>: indicator (IND).
- <*Data Type*>: <SENSOR>-<METHOD>. <SENSOR> is the primary remote sensing data source used to document the kinematics, in this case SENTINEL-1. <METHOD> is the primary method used to process the kinematic data, in this case INSAR.
- <*Product String*>: ROGIs for the product Rock Glacier Inventories.
- <*Additional Segregator*>: this should be structured as AREA_<REGION_NUMBER>-<AREA_NUMBER>. <REGION_NUMBER> follows the generic CCI Permafrost numbering: 5 – Carpathians (Romania), 6 – Western Alps (Switzerland), 7 – Troms (Norway), 8 – Finnmark (Norway), 9 – Nordenskiöld Land (Svalbard, Norway), 10 – Vanoise Massif (France), 11 – Southern Venosta (Italy), 12 – Disko Island (Greenland), 13 – northern Tien Shan (Kazakhstan), 14 – Brooks Range (Alaska, USA),

15 – central Andes (Argentina), and 16 – Southern Alps (Aotearoa New Zealand). <AREA_NUMBER> is a one- or multiple-digit number, depending on the numbers of area(s) in the region. For merged products (RoGIs in all areas), the additional segregator is ALL-AREAS.

- *<Layer Type>*: the individual layers of the vector product are provided in individual or merged files. The code of each individual layer is as follows.
  - AOI: extent of the RoGI area;
  - PM: layer 1, corresponding to the primary markers of the rock glacier units;
  - MA: layer 2, corresponding to the InSAR-based moving areas;
  - GO: layer 3, corresponding to the geomorphological outlines of the rock glacier units.

  The merged data package combining the different layers includes the three codes (PM-MA-GO).
- *<Indicative Date>*: format is YYYYMMDD, where YYYY is the year, MM is the month from 01 to 12, and DD is the day of the month from 01 to 31. Annual or multi-annual products are represented with YYYY only.
- *<fv File Version>*: file version number in the form n{1,} [.n{1,}] (two digits followed by a point and one or more digits).

Accordingly, the data package is structured as follows.

- The folder "ESACCI-PERMAFROST_ROGI_SINGLE-AREA", including the RoGI products for each area, for applications focusing on one specific region, with subfolders named as follows:
  - AREA_<AREA_NUMBER>_<AREA_NAME>_<COUNTRY_CODE>.
    Example: AREA_05-1_Carpathians_RO
    - AOI in a polygon vector layer in a gpkg format.
      Example: ESACCI-PERMAFROST-IND_SENTINEL1-INSAR_ROGI-AREA_5-1_AOI_2025-fv02.0.gpkg
    - Primary markers (PMs) in a point vector layer in a gpkg format.
      Example: ESACCI-PERMAFROST-IND_SENTINEL1-INSAR_ROGI-AREA_5-1_PM_2025-fv02.0.gpkg
    - Moving areas (MAs) in a polygon vector layer in a gpkg format.
      Example: ESACCI-PERMAFROST-IND_SENTINEL1-INSAR_ROGI-AREA_5-1_MA_2025-fv02.0.gpkg
    - Geomorphological outlines (GOs) in a polygon vector layer in a gpkg format.
      Example: ESACCI-PERMAFROST-IND_SENTINEL1-INSAR_ROGI-AREA_5-1_GO_2025-fv02.0.gpkg
- The file "ESACCI-PERMAFROST_ROGI_ALL-AREAS_AOI-PM-MA-GO_2025_fv02.0.gpkg", including the AOI and RoGI results (PMs, MAs, and GOs), merged for all areas, for applications requiring the combined use of all inventories.
- The file "AAA_README_FIRST.pdf" file describing the data structure and properties.

4 RoGI result description

Figure 4 is an example of the results of the RoGI multi-operator exercise for a selected area. It illustrates the similarities and differences between individual operator results (black dots for RGU PM; dashed lines for RGU GO) and the final products (coloured dots for RGU PM; solid lines for RGU GO). Due to the iterative and consensus-based procedure described in Sect. 2, the outcome is more than the sum of the individual results. The data package therefore includes the final consensus-based products only. In the following, we describe the results in each area separately (Sect. 4.1–4.12) before summarising the findings across all areas (Sect. 4.13).

4.1 RoGI area 5-1, RO (Carpathians, Romania)

RoGI area 5-1 is located in the Southern Carpathians in Romania (central lat and long location: 45°23′ N, 22°53′ E). The area covers an extent of approx. 18 km^2. The elevation ranges from peaks up to ∼ 2500 m a.s.l. along the southern mountain ridge to down to ∼ 1070 m a.s.l. in the valley further north.

Previous research showed sporadic and isolated patches of permafrost that are strongly linked with rock glaciers (Ardelean et al., 2015; Onaca et al., 2015; Popescu et al., 2024) and classified a small number of rock glaciers as active, with displacement rates on the order of cm yr^{-1} for the past decades (Necsoiu et al., 2016).

The multi-operator RoGI exercise resulted in the identification of 18 certain rock glacier units and 11 uncertain features. The InSAR-based MAs indicate velocities ranging from < 1 cm yr^{-1} to 3–10 cm yr^{-1}. The assigned KA has contributed to classify the RGU activity as relict (12 RGUs) and transitional (6 RGUs). The average size of the mapped rock glaciers is ∼ 0.07 km^2 based on the extended outlines.

4.2 RoGI area 6-1, CH (Western Alps, Switzerland)

RoGI area 6-1 is located in the upper part of the Réchy valley in the Western Swiss Alps (central lat and long location: 46°11′ N, 7°30′ E). The area covers an extent of approx. 12 km^2. The elevation ranges from peaks up to ∼

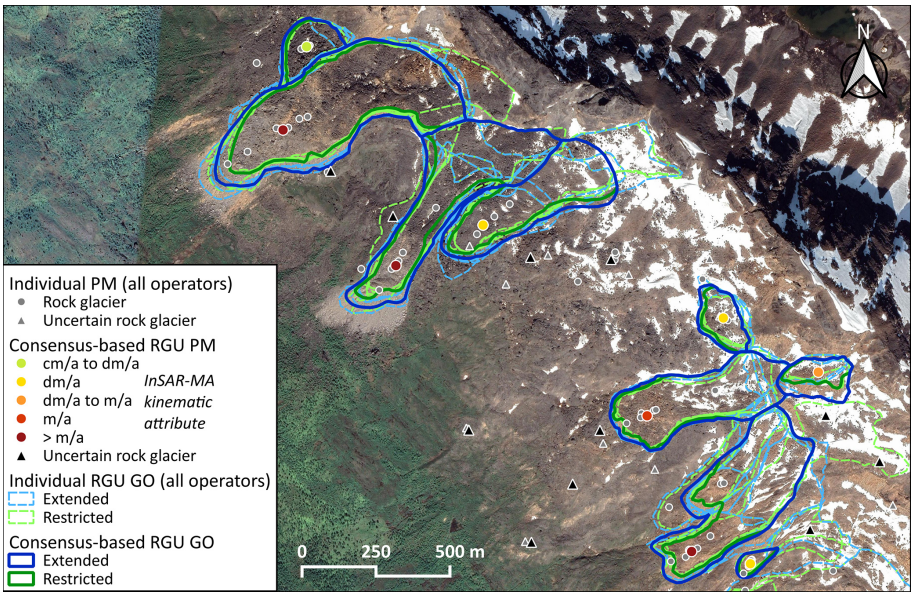

Figure 4. Example of RoGI results in part of area 7-1, NO-T (Troms, Norway), showing individual operator results and final consensus-based results (primary marker: PM; geomorphological outline: GO). For sake of visualisation, the MA layer is not shown but was used to assign the PM kinematic attribute displayed here on a green–red colour scale. See the example with MA in Fig. 3. Background: NorgeiBilde orthophoto (2016-08-2016).

3000 m a.s.l. along the southern mountain ridge to down to ∼ 2160 m a.s.l. in the valley further north.

Permafrost is still present in the upper part of the study area, whilst the lower area is mainly dominated by relict rock glaciers (Lugon and Delaloye, 2001; Marthaler et al., 2008; Tenthorey, 1992). The kinematics of the Becs-de-Bosson rock glacier has intensively been monitored since the early 2000s (Kellerer-Pirklbauer et al., 2024; PERMOS, 2024; Perruchoud and Delaloye, 2007) and displays velocities up to $2\,\mathrm{m\,yr^{-1}}$. Staub et al. (2016) used this site to evidence the dependency of the interannual variation in the rock glacier creep rate to the multi-year ground surface temperature forcing.

The multi-operator RoGI exercise resulted in the identification of 30 certain rock glacier units and 18 uncertain features. The InSAR-based MAs indicate velocities ranging from 1–3 $\mathrm{cm\,yr^{-1}}$ to $> 100\,\mathrm{cm\,yr^{-1}}$. The assigned KA has contributed to classify the RGU activity as relict (23 RGUs), transitional (4 RGUs), and active (3 RGUs). The average size of the mapped rock glaciers is $\sim 0.03\,\mathrm{km^2}$ based on the extended outlines.

4.3 RoGI area 7-1, NO-T (Troms, Norway)

RoGI area 7-1 is located in the Kåfjord–Storfjord mountainous region in Troms County, northern Norway (central lat and long location: 69°23′ N, 20°26′ E). The area covers an extent of approx. $47\,\mathrm{km^2}$. The elevation ranges from peaks up to ∼ 1400 m a.s.l. along the main Ádjit Mountain ridge to down to ∼ 400 m a.s.l. along the Skibotn valley flanks.

Previous research in this area indicated that the combination of seasonal frost and sporadic–discontinuous permafrost conditions in the region leads to a wide diversity of periglacial slope processes (Rouyet et al., 2021), including very high velocity rock glaciers (Eriksen et al., 2018). The distribution of relict and active rock glaciers fits the extents of the modelled Holocene and present-day permafrost extent in the region (Lilleøren et al., 2012).

The multi-operator RoGI exercise resulted in the identification of 15 certain RGUs and 26 uncertain features. The InSAR-based MA indicate velocities ranging from < 1 to $> 100\,\mathrm{cm\,yr^{-1}}$. The assigned KA has contributed to classify the RGU activity as transitional (4 RGUs), active (10 RGUs), and active uncertain (1 RGU). The average size of the mapped rock glaciers is $\sim 0.03\,\mathrm{km^2}$ based on the extended outlines.

4.4 RoGI area 8-1, NO-F (Finnmark, Norway)

RoGI area 8-1 is located along Store Skogfjorden and Hopfjorden in Finnmark country, northern Norway (central lat and long location: 70°45′ N, 27°50′ E). The area covers an extent of approx. $15\,\mathrm{km^2}$. The elevation ranges from peaks up to ∼ 535 m a.s.l. in the southeastern part to down the sea level along the fjord.

The area is located at the limit of the modelled regional permafrost extent (Gisnås et al., 2017). Although most past research has interpreted Finnmark rock glaciers as relict landforms (Lilleøren and Etzelmüller, 2011), a recent multi-

methodological study suggests that some rock glaciers at sea level are at a transitional stage (Lilleøren et al., 2022).

The multi-operator RoGI exercise resulted in the identification of 17 certain rock glacier units and 21 uncertain features. The InSAR-based MAs indicate velocities ranging from $< 1\,\mathrm{cm\,yr^{-1}}$ to 30–100 $\mathrm{cm\,yr^{-1}}$. The assigned KA has contributed to classify the RGU activity as relict (15 RGUs) and relict uncertain (2 RGUs). The average size of the mapped rock glaciers is $\sim 0.05\,\mathrm{km^2}$ based on the extended outlines.

4.5 RoGI area 9-1, NO-N (Nordenskiöld Land, Norway)

RoGI area 9-1 is located in the western part of Nordenskiöld Land on Spitsbergen, the main island of Svalbard (central lat and long location: 77°53′ N, 13°54′ E). The area covers an extent of approx. $10\,\mathrm{km^2}$. The elevation ranges from peaks up to ~ 900 m a.s.l. along the southeastern part of mountain ridge to down to ~ 50 m a.s.l. on the Nordenskiöldkysten strandflat.

Past rock glacier research in Svalbard identified low creep rates despite continuous permafrost and ice-rich conditions (Isaksen et al., 2000; Berthling et al., 1998). Along Nordenskiöldkysten, the apparent standstill of rock glaciers has been attributed to the low slope gradients where the rock glaciers flow onto the strandflat (Farbrot et al., 2005).

The multi-operator RoGI exercise resulted in the identification of 18 certain rock glacier units and 9 uncertain features. The InSAR-based MAs indicate velocities ranging from $< 1\,\mathrm{cm\,yr^{-1}}$ to 30–100 $\mathrm{cm\,yr^{-1}}$. The assigned KA has contributed to classify the RGU activity as relict uncertain (3 RGUs), transitional (9 RGUs), and active (6 RGUs). The average size of the mapped rock glaciers is $\sim 0.04\,\mathrm{km^2}$ based on the extended outlines.

4.6 RoGI area 10-1, FR (Vanoise Massif, France)

RoGI area 10-1 is located in the Vanoise Massif in France in the Western European Alps (central lat and long location: 45°19′ N, 6°37′ E). The area covers an extent of approx. $37\,\mathrm{km^2}$. The elevation ranges from peaks up to $\sim$ 3150 m a.s.l. in the southern part to down to ~ 1710 m a.s.l. in the valley further north.

Previous research in this area indicated that sporadic and discontinuous permafrost conditions in the region leads to a wide diversity and complexity of periglacial slope processes and several examples of rock glacier destabilisation (Marcer et al., 2021).

The multi-operator RoGI exercise resulted in the identification of 49 certain rock glacier units and 51 uncertain features. The InSAR-based MAs indicate velocities ranging from 1–3 $\mathrm{cm\,yr^{-1}}$ to $> 100\,\mathrm{cm\,yr^{-1}}$. The assigned KA has contributed to classify the RGU activity as relict (8 RGUs), relict uncertain (2 RGUs), transitional (13 RGUs), active (20 RGUs), and active uncertain (6 RGUs). The average size of the mapped rock glaciers is $\sim 0.03\,\mathrm{km^2}$ based on the extended outlines.

4.7 RoGI area 11-1, IT (Southern Venosta, Italy)

RoGI area 11-1 is located in Solda Valley (Suldental), a tributary valley of the Venosta Valley (Vinschgau), in western South Tyrol, Italy (central lat and long location: 46°33′ N, 10°36′ E). The area hosts two hanging valleys and covers an extent of approx. $19\,\mathrm{km^2}$. The elevation ranges from peaks up to ~ 3545 m a.s.l. for Cima Vertana in the eastern divide to down to ~ 2120 m a.s.l. further southwest.

According to a recently compiled geomorphological inventory, the area is characterised by the highest rock glacier density within South Tyrol ($\sim 1.1\,\mathrm{km^{-2}}$ against a regional average of $0.54\,\mathrm{km^{-2}}$) (Scotti et al., 2024). Subsequent integration of this geomorphological inventory with InSAR-based kinematic information across the Southern Venosta subregion led to detecting 375 intact and 428 relict rock glaciers (Bertone et al., 2024). On average, the velocity of intact rock glaciers was found to increase linearly with elevation up to the 2600–2800 m band (where mean annual air temperature declines from about -1 to $-2\,^{\circ}\mathrm{C}$), beyond which a kinematic plateau occurs. This band marks a broad altitudinal shift from transitional ($< \mathrm{dm\,yr^{-1}}$) to active ($> \mathrm{dm\,yr^{-1}}$) rock glacier types (Bertone et al., 2024).

The multi-operator RoGI exercise resulted in the identification of 39 certain rock glacier units and 13 uncertain features. The InSAR-based MA indicate velocities ranging from < 1 to $> 100\,\mathrm{cm\,yr^{-1}}$. The assigned KA has contributed to classify the RGU activity as relict (6 RGU), transitional (19 RGU), and active (14 RGU). The average size of the mapped rock glaciers is $\sim 0.05\,\mathrm{km^2}$ based on the extended outlines.

4.8 RoGI area 12-1, GL (Disko Island, Greenland)

RoGI area 12-1 is located along the northeastern coast of Disko Island, Greenland (central lat and long location: 69°51′ N, 52°33′ W). The area covers an extent of approx. $82\,\mathrm{km^2}$. The elevation ranges from peaks up to $\sim$ 1330 m a.s.l. mountain tops in the southwestern part to down at sea level.

There is a high density of rock glaciers in the area, previously explained by the combination of continuous permafrost and the abundance of heavily weathered basaltic bedrock (Humlum, 1996). Previous studies have already pointed out that tongue-shaped rock glaciers fed by glaciers in the hinterland are difficult to distinguish from debris-covered glaciers (Humlum, 1982).

The multi-operator RoGI exercise resulted in the identification of 29 certain rock glacier units and 19 uncertain features. The InSAR-based MAs indicate velocities ranging from < 1 to $> 100\,\mathrm{cm\,yr^{-1}}$. The assigned KA has contributed to classify the RGU activity as uncertain (2 RGUs), relict

(1 RGU), relict uncertain (9 RGUs), transitional (8 RGUs), and active (9 RGUs). The average size of the mapped rock glaciers is $\sim 0.05\,km^2$ based on the extended outlines.

4.9 RoGI area 13-1, KA (northern Tien Shan, Kazakhstan)

RoGI area 13-1 is located in the central part of Ile Alatau (also Zailiskiy Alatau), northern Tien Shan, in central Asia (central lat and long location: 43°0′ N, 77°1′ W). The area is located in southern Kazakhstan, close to the border with Kyrgyzstan. The area covers an extent of approx. $59\,km^2$. The elevation ranges from peaks up to ~ 4365 m a.s.l. in the eastern part to down to ~ 2570 m a.s.l. in the valley in the northwest.

Previous research has shown that rock glaciers are abundant in entire northern Tien Shan (Gorbunov and Titkov, 1989; Kääb et al., 2021; Titkov, 1988). More detailed investigations of the rock glaciers in the central part of northern Tien Shan highlighted the existence of several large complex rock glaciers, which originate in elevations where permafrost is very likely and flow down to elevations where permafrost is sporadic (Bolch and Gorbunov, 2014; Marchenko, 2001). Many rock glaciers in this region are highly active with average surface velocities of 1 to more than $2.5\,m\,yr^{-1}$ (Gorbunov et al., 1992; Kääb et al., 2021).

The multi-operator RoGI exercise resulted in the identification of 14 certain rock glacier units and 16 uncertain features. The InSAR-based MAs indicate velocities ranging from 1–3 $cm\,yr^{-1}$ to $> 100\,cm\,yr^{-1}$. The assigned KA has contributed to classify the RGU activity as transitional (1 RGU) and active (13 RGUs). The average size of the mapped rock glaciers is $\sim 0.35\,km^2$ based on the extended outlines.

4.10 RoGI area 14-1, US (Brooks Range, USA)

RoGI area 14-1 is located in the Brooks Range in northern Alaska, USA (central lat and long location: 68°6′ N, 149°58′ W). The area covers an extent of approx. $21\,km^2$. Elevation ranges from peaks up to ~ 2070 m a.s.l. in the central part of the area to down to ~ 1120 m a.s.l. in the valleys further north.

The area is underlain by continuous permafrost. Previous research in this area mapped rock glaciers between 900 and 2000 m a.s.l. and occurring mainly on the north side of the Brooks Range (Calkin, 1987; Ellis and Calkin, 1979; Ikeda et al., 2008). Previous measured rates of two rock glaciers in the 1980s were 10 and $40\,cm\,yr^{-1}$ (Calkin, 1987).

The multi-operator RoGI exercise resulted in the identification of 14 certain rock glacier units and 14 uncertain features. The InSAR-based MAs indicate velocities ranging from 1–3 $cm\,yr^{-1}$ to $> 100\,cm\,yr^{-1}$. The assigned KA has contributed to classify the RGU activity as relict (3 RGUs), transitional (2 RGUs), and active (9 RGUs). The average size of the mapped rock glaciers is $\sim 0.07\,km^2$ based on the extended outlines.

4.11 RoGI area 15-1, AR (central Andes, Argentina)

RoGI area 15-1 is located in the central Andes, west from Mendoza, Argentina (central lat and long location: 32°59′ S, 69.34° W). The area covers an extent of approx. $55\,km^2$. Elevation ranges from up to ~ 5530 m a.s.l. for the southernmost peaks to down to ~ 3570 m a.s.l. in the valley in the northern part of the area.

Previous studies reported an exceptional density of rock glaciers in the central Andes of Argentina (Zalazar et al., 2020), where permafrost occurs from ~ 3600 m a.s.l. upwards (Trombotto Liaudat, 2000). Recently, significant surface displacements between 0.37 and $2.61\,m\,yr^{-1}$ were assessed for large complex rock glaciers in the region (Blöthe et al., 2021), and short-term active layer monitoring documented the degradation of ice-rich permafrost in rock glaciers (Trombotto Liadat and Bottegal, 2019).

The multi-operator RoGI exercise resulted in the identification of 70 certain rock glacier units and 18 uncertain features. The InSAR-based MAs indicate velocities ranging from 1–3 $cm\,yr^{-1}$ to $> 100\,cm\,yr^{-1}$. The assigned KA has contributed to classify the RGU activity as relict uncertain (3 RGUs), transitional (19 RGUs), active (42 RGUs), and active uncertain (6 RGUs). The average size of the mapped rock glaciers is $\sim 0.12\,km^2$ based on the extended outlines.

4.12 RoGI area 16-1, NZ (Southern Alps, Aotearoa New Zealand)

RoGI area 16-1 is located in the Ben Ohau Range, part of the Southern Alps of Aotearoa New Zealand (central lat and long location: 43°59′ S, 170°3′ E). The study area covers an extent of approx. $7\,km^2$. Elevation ranges from peaks up to 2431 m a.s.l. for the highest peak in the north to down to $\sim$ 1600 m a.s.l. in the westernmost valley.

In 2 previous studies in the study area, Sattler et al. (2016) identified 2 relict, 4 inactive, and 6 active rock glaciers based on aerial image analysis only, while Lambiel et al. (2023) reported the presence of 10 transitional and 2 active rock glaciers using Sentinel-1 InSAR data.

The multi-operator RoGI exercise resulted in the identification of 24 certain rock glacier units and 6 uncertain features. The InSAR-based MAs indicate velocities ranging from 1–3 $cm\,yr^{-1}$ to > 10–$30\,cm\,yr^{-1}$. The assigned KA has contributed to classify the RGU activity as relict (9 RGUs), transitional (10 RGUs), and active (5 RGUs). The average size of the mapped rock glaciers is $\sim 0.03\,km^2$ based on the extended outlines.

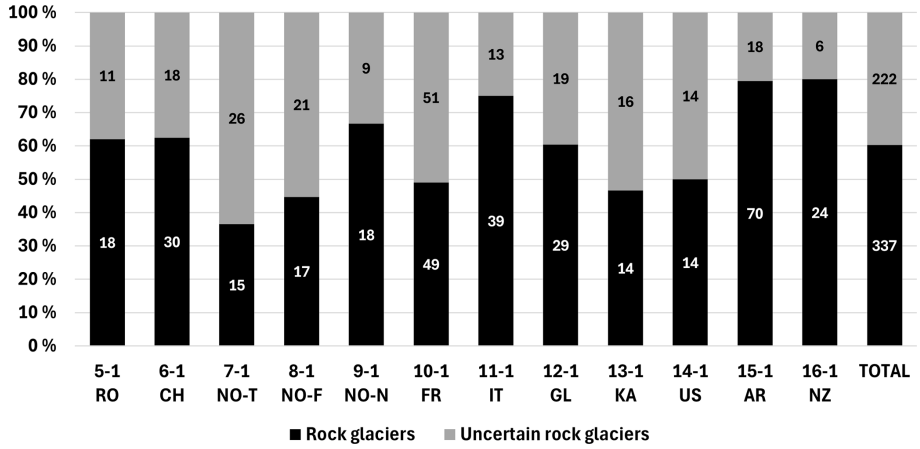

Figure 5. Relative distribution of the rock glacier units (RGUs) identified as "certain" (black) or "uncertain" (grey) in each RoGI area resulting from the consensus-based final primary marker (PM) layers. The numbers written in the bars correspond to the absolute numbers of landforms. The area numbers and the acronyms of the corresponding countries are in the *x* axis legend (RO: Romania, CH: Switzerland, NO: Norway (NO-T: Troms, NO-F: Finnmark, NO-N: Nordenskiöld Land), FR: France, IT: Italy, GL: Greenland, KA: Kazakhstan; US: USA; AR: Argentina, NZ: Aotearoa New Zealand), according to the naming convention in Table 1. Further analysis in the second phase of the exercise (outlining and characterisation of the attributes) was performed on the "certain" rock glaciers only.

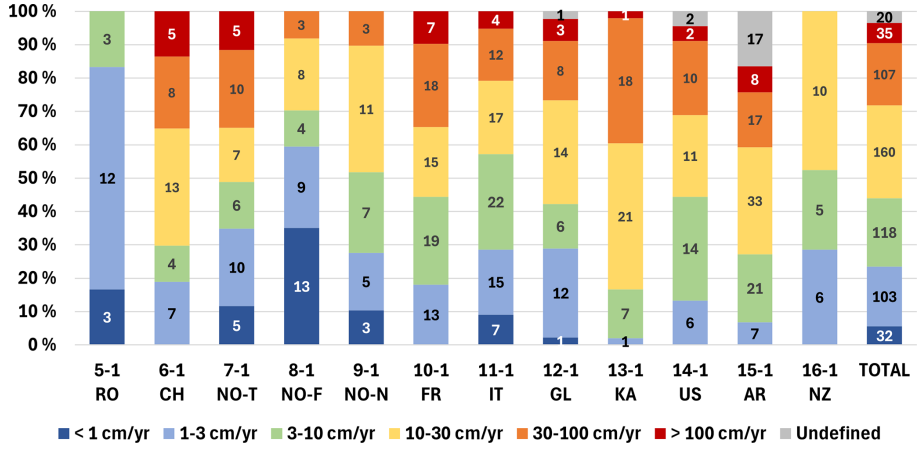

Figure 6. Relative distribution of the velocity classes of the InSAR-based moving areas (MAs) in each RoGI area resulting from consensus-based final MA layers. The numbers written in the bars correspond to the absolute numbers of landforms. The area numbers and the acronyms of the corresponding countries are similar to Fig. 5 and according to the naming convention in Table 1.

4.13 Result summary across all areas

In total, 337 "certain" rock glaciers were identified and characterised, and 222 additional landforms were identified as "uncertain" (Fig. 5). The level of uncertainty varies and reflects the geomorphological complexity of each area. On average, about 40 % of the landforms remain "uncertain". At these locations, the inventorying teams judged that we need more precise data and/or field visits to finalise the assessment.

The InSAR-based MA polygons have a wide range of velocities, both between and within the areas (Fig. 6). The MA layers were used to assign the kinematic attribute (KA) of each RGU, which then was used to assess the activity (Fig. 7). The kinematic and activity attributes of the PM files are therefore related to the MA layers, but the respective information is also complementary. While the activity is a convenient way to summarise the rock glacier state, the MA layers provide a more comprehensive overview of the distribution of the rock glacier creep rate. There are overall more MA polygons than RGU PM due to spatial heterogeneities in velocity (i.e. several MAs over the same RGU).

Based on the extended outlines, the RGUs have a typical size ranging between 0.01 and 0.25 km^2 (median value of each area, Fig. 8). The boxplots indicate large differences in size between and within the areas. It should be noted that in areas dominated by large rock glaciers (e.g. area 12-1 GL; area 13-1 KA), small talus-connected rock glaciers may have

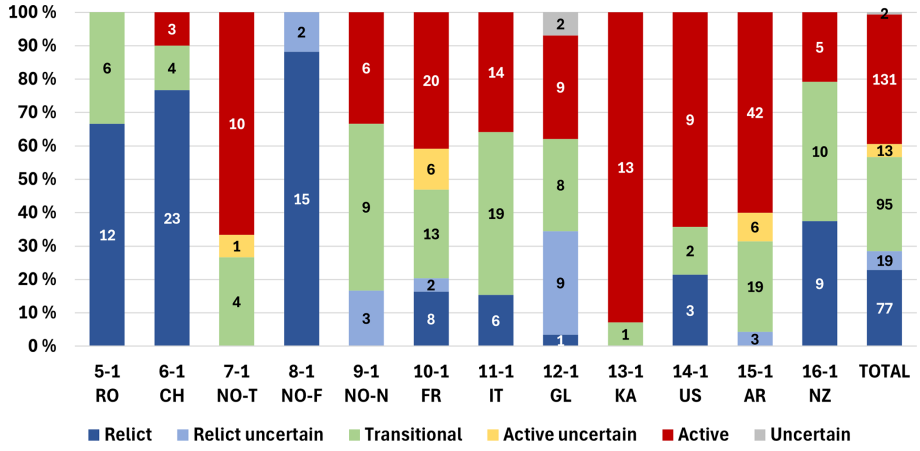

Figure 7. Relative distribution of the RGU activity (active, active uncertain, transitional, transitional uncertain, relict, relict uncertain, uncertain) documented as an attribute in the consensus-based final primary marker (PM) layers. The numbers written in the bars correspond to the absolute numbers of landforms. The area numbers and the acronyms of the corresponding countries are similar to Fig. 5 and according to the naming convention in Table 1.

been overlooked. The size of the areas significantly varies (ranging from 7 to 82 km^2; see Table 1). The size of the mapped landforms as well as the number of certain and uncertain RGU, in respect to the size of the area, are also highly variable (Fig. 9). Some areas are characterised by many small landforms (e.g. area 6-1 CH and area 16-1 NZ), while others are dominated by a few large rock glacier units (e.g. area 12-1 GL and area 13-1 KA).

5 Uncertainties and limitations

5.1 Documentation of uncertainties and limitations

In the attribute tables of the three GeoPackage files, various fields document the reliability of the mapping and morphokinematic assessment according to identified uncertainties and limitations:

- For the PM files, the attribute "uncertain" describes ambiguous areas that should be investigated in the future (need for additional data and/or field visit). For educational purposes, the attribute "not a rock glacier" could also be used to highlight landforms that are likely to be misinterpreted as rock glaciers. The level of uncertainty and complexity can be highlighted for many morphokinematic attributes, either in the selectable categories (for example "active uncertain", "transitional uncertain", and "relict uncertain" for the attribute "Activity") or using an additional reliability attribute for the kinematic assessment (Appendix A). Additional comments describing the uncertainty sources and ambiguities in the interpretation can be written in two "Comment" fields.
- For the MA files, the reliability (or the degree of confidence) of the results is qualitatively documented in accordance with the quality of the detection, the delineation of the moving areas based on the available InSAR data, the signal interpretation, and the resulting velocity estimation (Appendix B). When medium–low reliability is set (uncertain InSAR signal and/or unclear MA outlines), information on the uncertainty sources and ambiguities in the interpretation can be described in a "Comment" field.
- For the GO files, the reliability of the delineation at different locations of the rock glacier (front, left/right lateral margins, upslope boundary) is estimated with a score of 0 (low), 1 (medium), or 2 (high). It consists of a qualitative assessment depending on the data quality and the geomorphology complexity of the landform (Appendix C). The automatic summation of the scores (0–8) gives a general estimate of the outline reliability for the entire landform. Information regarding the data source(s) used for the delineation and the uncertainties impacting the reliability of the resulting polygon can be documented in a "Comment" field.

5.2 Summary of uncertainties and limitations for each RoGI product

Here we summarise the observations about the uncertainties and limitations of the 3 output files based on the results in the 12 areas and the feedback of the operator teams. Most challenges are common for all areas, while a few affect specific areas only. The main identified uncertainties and limitations of each output product are described in the following sections and summarised in Table 3. Despite the effort to stan-

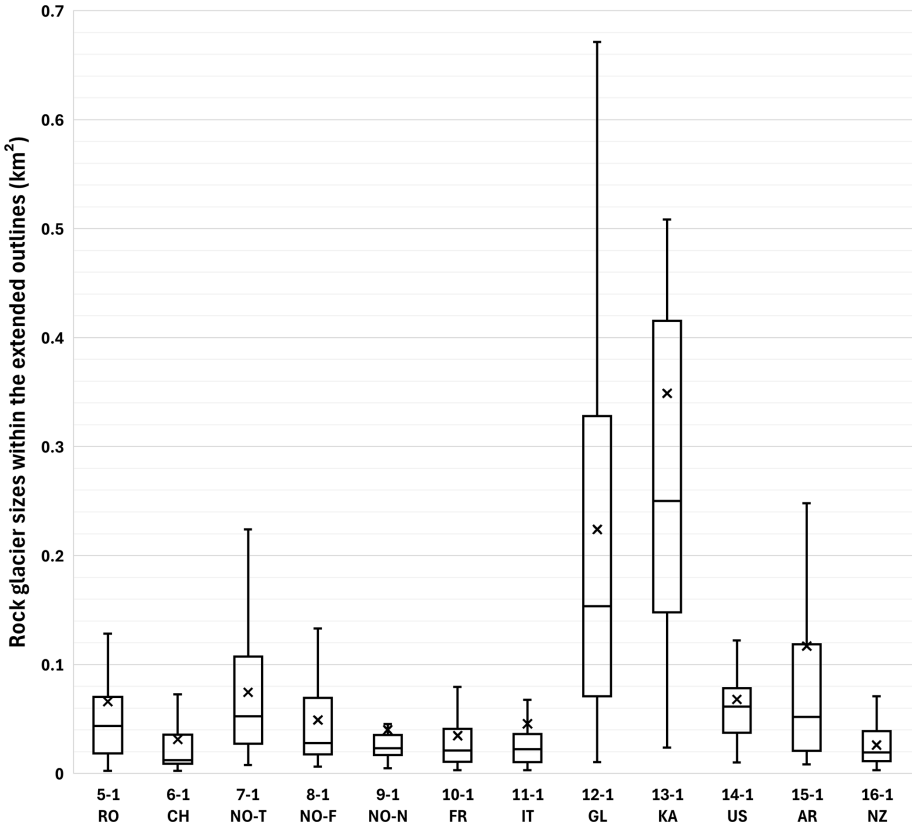

Figure 8. Range of RGU sizes within the extended geomorphological outlines (GOs) in each RoGI area resulting from the consensus-based final GO layers. The horizontal lines in the boxes indicate the median values. The lower and upper limits of the boxes indicate the first and third quantiles. The whiskers highlight the maximum and minimum values. The crosses indicate the averaged sizes. The area numbers and the acronyms of the corresponding countries are similar to Fig. 5 and according to the naming convention in Table 1.

dardise the procedure and reduce the differences between the areas, we acknowledge that discrepancies remain in the final products. These are due to the different levels of geomorphological complexity; the variable numbers of landforms and the density of their distribution; as well as the heterogeneous data quality, local knowledge, and research history. In the case of operator discrepancies, the decisions were taken at the team level, ensuring homogeneity within each area. Major questions were discussed during PI coordination meetings and communicated across the teams thanks to operators working in several areas. The parallel timeline of the work in all areas contributed to a good communication on the common challenges but did not discard all risks of inter-regional differences and subjective treatment.

5.2.1 Uncertainties and limitations of the PM products

– The quality of the PM products depends on the availability, resolution, and quality of the source data, which vary among the areas. Optical imagery affected by shadows, clouds, or snow cover led to increased uncertainty in some areas. Warm regions in the marginal permafrost zone can be dominated by relict landforms with dense vegetation cover that may hinder detailed mapping based on passive optical remote sensing only. In such areas, terrain hill shades from a high-resolution lidar DEM are highly valuable as complementary input data. The availability and quality of such products vary, however, from one region to another. In areas dominated by large glacier-connected or glacier-forefield-connected rock glaciers, small talus-connected rock glaciers tended to be overlooked, which may explain the different size distribution between the areas (see Fig. 8). The identification of small and relatively shallow rock glaciers developed on debris-mantled slopes was challenging, as they often do not exhibit well-defined rooting zones and lateral margins.

– InSAR was useful for detecting rock glaciers that may have been missed when only looking at optical images. However, it also added an additional source of variability between the regions because the data availability and properties vary from one region to another (Table 2). In

Table 3. Overview of the main uncertainties and limitations of the RoGI products and how they apply to the 12 areas. The crosses (X) show where the problem has been explicitly reported by the RoGI team/PI. The circles (O) show where the problem might happen for specific landforms but was not reported as a main limitation by the RoGI team/PI. The area numbers are similar to Fig. 5 and according to the naming convention in Table 1.

	5-1	6-1	7-1	8-1	9-1	10-1	11-1	12-1	13-1	14-1	15-1	16-1
PM detection and characterisation												
Optical imagery affected by shadows, clouds, snow	O	O	O	O	X	O	O	X	O	X	O	O
Dense vegetation cover on relict rock glaciers	X											
Dominance of large RGU and small RGU likely overlooked								O	X	X	X	
Ambiguous imbrication of periglacial landforms	O	O	X	X	O	X	O	O	O	X	O	
Ambiguous rock glacier and glacier/forefield continuum	O	X	O	O	O	O	O	O	X	X	X	
Variable categorisation of landslide-connected RGU	O	O	X	O	O	X	O	O	O	O	O	
Difficulty with selecting RGU for complex multi-unit systems	O	O	X	O	O	O	O	O	X	X	X	O
Ambiguity in activity in Arctic cold regions with slow/no MA					X		O		O			
Difficulty with discriminating active/transitional		O	O		O	O	O	O	O	O	O	X
MA detection, delineation, and characterisation												
Fewer available Sentinel-1 images and longer repeat-pass								X	X	X	X	X
Challenge of velocity estimate for operators with little InSAR experience	X	X	X	X	X	X	X	X	X	X	X	X
Difficulty with documenting and interpret small and slow MA	X	O	O	X	O	O	O	O	O	O	O	O
Difficulty with discriminating creep from other processes	O	O	O	X	X	O	O	X	O	X	O	O
GO delineation and characterisation												
Uncertainty in the delineation of the upper boundaries	X	X	X	X	X	X	X	X	X	X	X	O
Uncertainty in the delineation of eroded, reworked or exaggerated fronts	X	X	O	X	O	X	X	O	O	X	X	O
Unclear lateral margins for small rock glaciers	O	O	O	X	O	O	X	O	O	O	O	O
Difficulty with outlining complex RGSs with multiple RGUs	O	O	X	O	O	O	O	O	X	X	X	O
Variable quality of optical imagery and georeferencing shifts	O	O	O	X	X	O	O	X	X	X	O	O

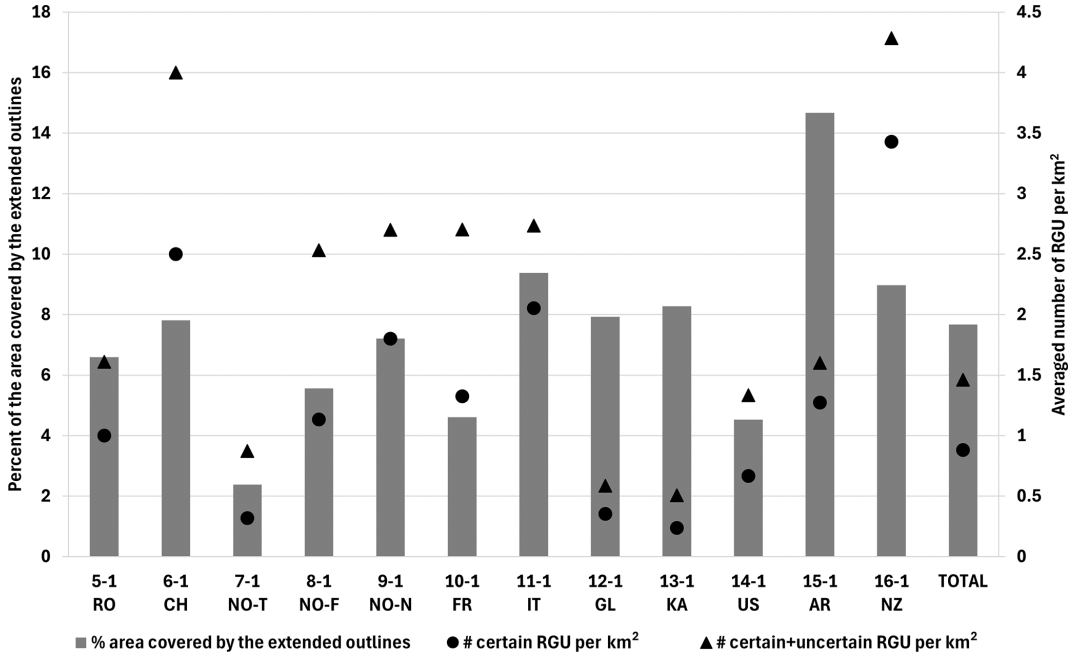

Figure 9. Density of rock glaciers in the studied areas. The grey bars show the percentage of the area covered by rock glaciers according to the mapped extended outlines. The corresponding values are shown on the primary vertical axis on the left. The black symbols (dots: certain rock glaciers, triangles: certain and uncertain rock glaciers) show the numbers of identified RGUs in respect to the size of the area (number per km^2). The corresponding values are shown on the secondary vertical axis on the right. The area numbers and the acronyms of the corresponding countries are similar to Fig. 5 and according to the naming convention in Table 1.

areas with multi-temporal PS/DS InSAR data, the detection capability to low velocity was increased. In areas with X-band SAR data, interferograms with higher spatial resolution were provided, which allowed for detecting smaller moving landforms. In areas with L-band SAR data and 6 d Sentinel-1 repeat pass, the maximal detection capability was increased.

– The level of geomorphological complexity and the interactions with other glacial and periglacial processes vary among the areas. Several teams reported the challenges of discriminating landforms due to the glacier–rock glacier continuum or between rock glacier landforms and complex morainic systems in the case of rock glaciers derived from a former (late-glacial) glacier forefield. The imbrication with other types of periglacial processes also leads to ambiguities in landform discrimination (e.g. large coarse solifluction lobes and rockslide deposits). In such cases, the final products include many "uncertain" PMs and several cases with unclear upslope connections. In areas with landslides, there were difficulties in assigning the type of upslope connection. The "landslide-connected" upslope unit is somewhat ambiguous as it often practically means that there is a poly-connection (talus + landslide). In such cases, the high level of discrepancy between operators required some discussions to agree on a final category.

– One challenge reported by all teams is related to the variable level of details applied to discriminate landforms with complex morphology. There were discrepancies among the operators in the way to interpret multi-unit systems and discriminate the units. In complex cases, some operators considered the landforms as one main complex unit (one PM), while others identified several units (several PMs). After discussions, consistent solutions were found within each area. There are remaining differences between the areas due to the variable geomorphological complexity.

– The quality of the attribute characterisation depends on the complexity of the study area. In cold-climate regions with continuous permafrost, one challenge is related to the kinematic and activity attributes. Although the landforms are "active" in the traditional sense (i.e. intact, with the presence of permafrost), some are very slowly creeping and so fall into the transitional or relict category according to the current RGIK definition (low efficiency of sediment conveyance). The activity is also challenging to assess in areas where the contrast in surface material between the rock glacier surface and the front is generally low. In such cases, the front is generally smooth, which makes it hard to discriminate active from transitional rock glaciers without kinematic information.

5.2.2 Uncertainties and limitations of the MA products

- The accuracy of the kinematic analysis varied between areas due to unequal data availability. Some areas had a variety of InSAR data from different SAR sensors and processed with different algorithms (single interferograms, stacking and PSI), providing a wide range of detection capabilities. In such cases, the areas with no MA could reliably be interpreted as "no movement" (i.e. movement $< 1\,\mathrm{cm\,yr^{-1}}$) and high to very high velocity can be discriminated ($30–100\,\mathrm{cm\,yr^{-1}}$ or $> 100\,\mathrm{cm\,yr^{-1}}$). However, some areas had fewer datasets and longer Sentinel-1 repeat-pass time interval (extra-European areas), which led to reduced maximal detection capability. Using Sentinel-1 12 d repeat-pass only, it is not possible to discern $30–100\,\mathrm{cm\,yr^{-1}}$ and $> 100\,\mathrm{cm\,yr^{-1}}$, which leads to discrepancies in the way to assign the $\mathrm{m\,yr^{-1}}$ and $>\mathrm{m\,yr^{-1}}$ categories (kinematic attribute in the PM layer).

- The InSAR interpretation resulted in discrepancies between operators. All teams reported that it was the hardest step of the RoGI procedure due to variable backgrounds of the operators. A consensus-based process was difficult to perform due to variable levels of experience with InSAR, different ways of looking at all available datasets, and variable levels of details in systematically outlining the MAs. In most cases, the same MAs were similarly identified and delineated, but the velocity classes were sometimes assigned differently. Despite this challenge, many operators reported that the work was highly educative, and all teams had at least one operator well experienced with InSAR, which ensured high quality in the final results.

- In general, major fast-moving MAs were detected with few variabilities among operators, while small and slow MAs were more difficult to interpret. In marginal permafrost zones, there is a dominance of transitional and relict rock glaciers characterised by little (or no) movement. The MAs are small and with low velocity and therefore hard to identify compared to other areas characterised by strong InSAR signal on interferograms with short time intervals between the compared images. The documentation of low-velocity MAs requires the availability of multi-temporal PS/DS data with other properties and interpretation constraints, compared to single interferograms.

- A general challenge with InSAR analysis is to ensure that the detected movement is representative of the rock glacier creep rate and not significantly affected by other processes (e.g. landslide, solifluction, and thaw subsidence). Analysing a diverse set of interferograms (various SAR geometries, time intervals, months, and years) allows us to reduce the risk of misinterpretation by providing complementary information about the spatial and temporal characteristics of the movement pattern. However, we cannot fully discard the possibility that some MAs identified on a rock glacier might be affected by other processes. In the case of rapid permafrost degradation, the detected movement may correspond to a mixed signal from downslope creep and subsidence due to ice core melt. In cold regions with continuous permafrost, the ground is highly dynamic during the thawing season, which makes it difficult to dissociate the InSAR signal on the rock glacier from surroundings areas that also move. When analysing small and slowly creeping talus-connected rock glaciers, it was sometimes challenging to discriminate the movement associated with rock glacier creep from other processes, such as thaw subsidence in ice-rich lowlands located directly at the foot of the mountain ridges.

5.2.3 Uncertainties and limitations of the GO products

- The main difficulty was to delineate the upper boundary between the rock glacier and its contributing area, depending on the type of upslope connection. For glacier-connected or glacier-forefield-connected rock glaciers, the location of the upper boundary was often ambiguous, and the corresponding outline reliability is therefore set to "low" in the attribute table. For talus-connected rock glaciers, there were discrepancies regarding how to draw the upper outline: straight line on the upslope area of the rock glacier versus a curved connection to avoid the inclusion of talus cones feeding the rock glacier. The teams discussed this challenge and agreed on drawing a curved line, continuing the delineation of the front and margins while following the topography. When the location of the boundary was uncertain, the upper outline reliability was set to "low" or "medium" in the attribute table.

- In some cases, the delineation of the front was challenging, especially if the toe of the rock glacier was reworked by other processes, such as solifluction. Smooth fronts and rounded ridges and furrows, often associated with relict and transitional landforms, may lead to ambiguous delineation of the restricted outlines. For a rock glacier developing on a steep slope, the front may also be difficult to distinguish. Some problems were, for instance, identified in cases of exaggerated fronts blended with the downside talus slope. Small rock glaciers, such as debris-mantled connected rock glaciers, or embryonic talus-connected landforms (protalus ramparts) often had ambiguous lateral margins, challenging for outlining. Such complicated cases were discussed during team meetings to find a mutually agreed-upon solution. When the location of the boundary was uncertain, the

front and/or lateral outline reliability was set to "low" or "medium" in the attribute table.

- Complex rock glacier systems with several units were the most challenging landforms to outline. The delineation was especially difficult in the case of adjacent landforms or several generations of partly overlapping rock glacier units. In some cases, several units initially identified with different PMs in the first phase of the exercise were not outlined separately in the second phase (too complex). The two phases (PM identification and GO delineation) were performed iteratively. When the outlining process highlighted that multi-unit discrimination was bringing too much uncertainty, the PM numbers and locations were revised (simplification).

- Combining different data sources with variable acquisition times, snow/vegetation covers, and sunlight directions helped interpreting and mapping some rock glaciers. On the other hand, some areas are affected by georeferencing shifts between the different optical data sources available in the online services. These shifts may explain some discrepancies among operators, depending on the main source used to digitalise the boundaries. The scale and level of detail used to perform the outlining work also varied between the operators. This challenge did not affect the consistency and quality of the final products that were discussed within the teams and accordingly revised by each PI. The data source used for the final outlines and the time it applies are specified in the attribute table. The results apply for the period during which the outlines were drawn. If viewing the results with a more recent background imagery, new shifts may occur due to the regular updates of the WMS data sources and their variable quality.

5.3 Quality assessment of the multi-operator RoGI procedure

Here we summarise the observations about the multi-operator RoGI procedure based on the results in the 12 areas and the feedback of the operator teams.

5.3.1 Value of the RoGI exercise and the multi-operator procedure

- The steps and instructions of the exercise were generally assessed as clear and easy to follow. The operators reported that they liked the structure and clarity of the provided GIS and data packages. Thus, it is a promising endeavour to apply the same structure in new regions and therefore ensure consistency in future RoGI data compilation.

- Each team had two multi-operator meetings with 3–10 people attending. The size of the teams proved ideal for such an exercise as more people would have been challenging to manage and ensure efficient discussions. In some cases, the digital meetings were complemented with email interactions (e.g. sharing comments in documents, print-screen images, and presentations and sending recordings of meetings). All types of communication were found valuable, both for a personal learning purpose and for improving the quality of the final products.

- Having operators with different skills and backgrounds was found to bring in added value to the final results. The combination of different points of view and experiences from several regions around the world ensured that various morpho-kinematic elements were identified and taken into consideration.

- Although InSAR interpretation has been identified as the most challenging step due to little experience for some operators, several teams report that the data were valuable at different levels. InSAR was useful for identifying moving rock glaciers in addition to providing a semi-quantitative information about their creep rates. When used iteratively with PM detection (Fig. 2), the MA step allowed for including landforms that would have been overlooked based on geomorphological criteria only. It was especially valuable in areas where optical imagery was affected by shadows, clouds, or snow cover.

5.3.2 Challenges and suggestions to improve the RGIK procedure and guidelines

- The consensus-based procedure generally worked well for the PM identification, the GO delineation, and the categorisation of key attributes (e.g. upslope connection, kinematics, and activity). However, some steps cannot be comprehensively assessed during team meetings. It is, for example, not feasible to collectively discuss all details of the InSAR interpretation. Practically, the PIs compared their own results with those of the other operators and corrected their results when mistakes were found. A comprehensive consensus-based process can work but only on a small set of rock glaciers, which could then be used for adjusting the assessment criteria before upscaling.

- The InSAR interpretation was challenging for operators without past experience with these types of data. Despite discrepancies in the quality of some individual results, that issue did not impact the final products as each team included at least one person with InSAR experience. Nevertheless, the teams suggested various ways to improve this part in the future, such as (1) adding new examples in the guidelines on how to read the interferograms; (2) splitting the multi-operator process into two

separate teams (one with InSAR expertise focusing on the MA part, one with geomorphological expertise focusing on the PM/GO and using the final MA for the kinematic assessment); and (3) pre-processing the data and providing the velocity products in formats that are easier to interpret by non-experts.

- The assignment of the activity attribute based on geomorphological and/or kinematic criteria requires clarification in the guidelines. The InSAR analysis led to the generation of a MA layer with polygons highlighting where movement has been detected. For characterising the kinematics and the activity, the operators used the MA layer as input. However, some rock glaciers are not covered by an MA. In such cases, it was recommended to avoid overinterpreting the absence of detected movement because a rock glacier without an MA may mean two different things: (1) there is no movement, or it is too low to be detected, or (2) the data quality and/or coverage did not allow for detecting it. In such cases, some operators only focused on geomorphological criteria to assign the activity. A kinematic attribute with a low velocity and low reliability index may have been documented but was not used to set the activity. For other operators, the lack of movement evidence has been used in synergy with geomorphological evidence as an additional indicator confirming the geomorphological interpretation.

- As part of the GO step, the upper outline between rock glacier and its contributing area was identified as the most challenging part to delineate. The way to draw the upper outline when there is a high level of uncertainty could be improved in the RGIK guidelines, based on additional examples, for different landform types and from different places around the world. The scale of digitalisation was not specified at the beginning of the exercise, which led to discrepancies in outlining the level of detail and size of the considered landforms. The way to document the data source, imagery date, and scale of analysis could be improved. When using Bing, Google, or ESRI WMS imagery, it is important to specify the main data source and the date the work has been performed as these open services have differences and frequent updates, which lead to GO shifts. It was encouraged to do it in the "Comments" or "Kin.Comments" fields, but other elements could be written in these fields, which led to variable metadata documentation depending on the operator.

- Several operators commented that there were many variables to document. The entire inventory process was consequently time-consuming, which led to variable levels of detail. It should be noted that in the framework of this exercise, all steps were required, although several elements are presented as "optional" in the guidelines. For example, the GOs are valuable but are not mandatory to draw. A combination of PMs with and without GOs is possible within the same RoGI. One could decide to delineate a large system and mark the locations of several units using PMs only (i.e. without outlining at the same level). More compact versions of the RoGI protocol could be developed to avoid discouraging some groups to follow it. Alternative ways to summarise the essential information contained in the RGIK guidelines (short checklist document, flowchart with a link to necessary definitions, video tutorial, etc.) may also help RoGI operators to have a quick overview of the main tasks to perform.

Overall, despite discrepancies in the individual results, the above issues did not impact the final products. Consistent solutions were found after discussions within and among the team(s).

6 Data availability

The final PM/MA/GO dataset is available on Zenodo (Rouyet et al., 2025; https://doi.org/10.5281/zenodo.14501398). The GeoPackage (gpkg) templates for performing similar RoGI in other areas, and exercises based on the QGIS tool are available on the RGIK website (RGIK, 2025, https://www.rgik.org/resources/). The data can also be viewed in a dedicated WebGIS tool (https://bigweb.unifr.ch/Science/Geosciences/Geomorphology/Pub/Website/CCI/CCI_qgis2web_2025_04, UNIFR, 2025).

7 Conclusion: potential use and applications

The multi-operator RoGI exercise was performed in 2023 and involved 41 people who applied the RGIK guidelines in 12 areas spread around the world. This unique international initiative fulfilled the four initial objectives outlined at the end of Sect. 1. First, we demonstrated that it was feasible to apply common RoGI guidelines and procedures in various mountainous environments. All teams acknowledged that the initiative was highly instructive thanks to the lively discussions in team meetings, the diversity of backgrounds and experiences, and the possibility of performing the work in various geomorphological contexts. Second, we identified various limitations (see Sect. 5) that will serve to improve the RGIK guidelines in the future. Third, we developed standardised GIS templates for homogenising the production of future RoGIs and providing training tools for the community. The GIS templates and two online exercises are already available on the RGIK website. Fourth, we compiled and disseminated a homogenised set of RoGIs in 12 diverse regions.

The resulting dataset has the potential to be used for several applications. Here we discuss four potential uses.

- *Further investigation in the selected areas and RoGI upscaling:* the exercise was performed on relatively small areas (7–82 km^2) to make it feasible to apply the demanding procedure described in Sect. 2. All PIs and involved research groups acknowledged the educational value of the process and that the lessons learnt during the exercise will contribute to continuing their work in the regions, with the long-term objective being to upscale the RoGIs to entire mountain ranges. The landforms, for which the current characterisation was uncertain with the applicable data, may be investigated further during future targeted fieldwork campaigns or when new datasets become available.

- *Rock glacier selection for rock glacier velocity (RGV) monitoring:* following the recent acceptance of RGV as a new parameter of the ECV Permafrost (Hu et al., 2025; Streletskiy et al., 2021; WMO, 2022), one important task of the community is to monitor the interannual velocity changes of selected rock glaciers using in situ and/or remote sensing techniques. It is highly recommended to have a good understanding of the rock glaciers selected for long-term monitoring and exploitations as climate change indicator. The development of comprehensive RoGIs in several regions is therefore a valuable first step to design monitoring strategies in each area (RGIK, 2023c).

- *Educational training tools for enhancing the systematic generation of RoGIs worldwide:* the international multi-operator exercise highlighted the variety of rock glacier morphologies and characteristics across the selected mountain ranges, showing the importance of illustrating the RGIK guidelines with examples from different regions. The operator comments show the need to promote the guidelines with alternative tools (e.g. compact version of the RoGI protocol, short checklist document, flowchart summarising the main steps with links to necessary definitions, video tutorial, and additional GIS training tools based on the present dataset). New training material, partly based on our RoGI dataset, may contribute to promoting and supporting the generation of RoGIs in under-studied regions.

- *Training data for automated inventorying techniques:* there is growing interest in the community for developing automated solutions for RoGI generation at a large scale using machine learning (Erharter et al., 2022; Mahanta et al., 2024; Robson et al., 2020; Sun et al., 2024). Per definition, machine learning requires high-quality datasets to train the model. Transferability is typically a challenge. If the input data are clustered in a small area, the model may fail to map rock glaciers in another region with different conditions. In this respect, despite the few landforms in each area, our dataset covers a wide range of topographic, geological, and climatic conditions. To our knowledge, this is the first publicly released dataset that combines RoGIs in 10 different countries and on 5 continents, which will hopefully be valuable for machine learning applications.

Appendix A: Attribute table of the primary marker (PM) files

Table A1. Attributes of the primary marker (PM) gpkg files (M: mandatory attribute, O: optional attribute). The table only includes the essential definitions necessary to understand the overall meaning of the attributes. The last column refers to the sections of the RGIK guidelines documenting the detailed recommendations for identifying rock glaciers and assigning values to each attribute. At the time of the exercise, the table referred to the sections of several dedicated documents (RGIK, 2022a, b, c). The RGIK RoGI guidelines have since been merged into one reference document (RGIK, 2023a). The following table has therefore been updated accordingly.

Attribute	Description	Values	RGIK guidelines
fid (M)	Unique identifier of the primary marker.	Automatic filling	
Landform (M)	"Rock glacier" is the default value. "Uncertain rock glacier": ambiguous landforms that should be investigated in the future (need for additional data and/or field visit). It provides an option to document the location of suspected rock glaciers that remain uncertain based on the currently available data. "Not a rock glacier": this attribute allows the operators to highlight landforms that are likely to be misinterpreted as rock glaciers, for educational purpose.	0. Uncertain rock glacier 1. Rock glacier 2. Not a rock glacier	RoGI guidelines, Chap. 3 (Sect. 3.1 and 3.7) RoGI guidelines, Chap. 5 (Sect. 5.1) https://doi.org/10.51363/unifr.srr.2023.002
WorkingID (O)	Practical identifier chosen by the operator (e.g. TYR001 and TYR002 for an inventory in Tyrol).	Text	
Lat (M)	Latitude of the primary marker in decimal degrees.	Automatic filling	
Long (M)	Longitude of the primary marker in decimal degrees.	Automatic filling	
PrimaryID (M)	RGU + 12 to 15 digits depending on the "lat" and "long" values. Always four digits after the degrees. (e.g. RGU34567S123456E means 3,4567° S and 12,3456° E).	Automatic filling	RoGI guidelines, Chap. 5 (Sect. 5.2) https://doi.org/10.51363/unifr.srr.2023.002
Alter.ID1 (O)	Alternative local or regional name.	Text	
Alter.ID2 (O)	Identifier used in a previous inventory.	Text	
Assoc.RGS (O)	Defines if the primary marker is part of a mono-unit system ("Mono-unit RGS") or a multi-unit system ("Multi-unit RGS"). "Mono-unit RGS": a rock glacier system (RGS) including only one unit. "Multi-unit RGS": a rock glacier system (RGS) composed of multiple units that are spatially connected either in a downslope sequence or through coalescence.	1. Mono-unit RGS 2. Multi-unit RGS	RoGI guidelines, Chap. 3 (Sect. 3.2) https://doi.org/10.51363/unifr.srr.2023.002
RGS.Primar (O)	Primary ID of the associated rock glacier system. RGS + 12 to 15 digits depending on the "lat" and "long" values. Always four digits after the degrees.	Automatic filling	
Morpho. (O)	Defines if the rock glacier identified by the primary marker is a rock glacier with simple or complex morphology. "Simple": unambiguous and homogeneous morphological expression and/or land cover and connection to the upslope unit and activity (or kinematic if available). "Complex": ambiguous and heterogeneous morphological expression and/or land cover and connection to the upslope unit and activity (or kinematic if available). Despite the spatial variability, there is no sufficient evidence to unambiguously separate units.	1. Simple 2. Complex	RoGI guidelines, Chap. 3 (Sect. 3.2) RoGI guidelines, Chap. 5 (Sect. 5.3) https://doi.org/10.51363/unifr.srr.2023.002

Table A1. Continued.

Attribute	Description	Values	RGIK guidelines
Complet. (O)	Defines if the rock glacier identified by the primary marker is completely visible or not. "No, Ups.Con" means that it is not complete due to an unclear upslope connection (e.g. several rock glaciers generations are overlapping). "No, truncated front" means that it is not complete due to a truncated front. "Uncertain" when data or analysis does not allow for a decision.	1. Yes 2. No, unclear connection to the upslope 3. No, truncated front 4. Uncertain	RoGI guidelines, Chap. 5 (Sect. 5.3) https://doi.org/10.51363/unifr.srr.2023.002
Upsl.Con. (O)	Defines the geomorphological unit directly located upslope of a rock glacier unit or system (five main categories). See related documentation for further information. When dealing with uncertain or intermediate situations, four additional categories are included: "poly-connected", "other", "uncertain", and "unknown". "Poly-connected": two or more upslope connections (e.g. talus and glacier). The use of poly-connected should be restricted to cases where there is no obvious dominance of one connection type. "Other": other types of geomorphological sequencing related to a rock glacier landform. "Uncertain": the geomorphological assessment cannot be performed with confidence. "Unknown": the rock glacier unit has been overridden by another one, and the former connection to the upslope unit cannot be assessed with confidence anymore.	1. Talus-connected 2. Glacier-forefield-connected 3. Glacier-connected 4. Debris-mantled slope-connected 5. Landslide-connected 6. Poly-connected 7. Other 8. Uncertain 9. Unknown	RoGI guidelines, Chap. 3 (Sect. 3.3) RoGI guidelines, Chap. 5 (Sect. 5.3) https://doi.org/10.51363/unifr.srr.2023.002
Upsl.Cur. (O)	Defines if the rock glacier is currently connected to the upslope unit or not. This attribute is noted only for "talus-connected" rock glaciers and allows rock glaciers that are currently connected to their upslope unit (i.e. efficient sediment connectivity) to be distinguished from those that have been disconnected from their original source.	1. Yes 2. No 3. Uncertain 4. Unknown	RoGI guidelines, Chap. 3 (Sect. 3.3) RoGI guidelines, Chap. 5 (Sect. 5.3) https://doi.org/10.51363/unifr.srr.2023.002
Comment (O)	Comment on possible poly-connection and uncertainty in the geomorphological interpretation.	Text	
Acti.Ass. (O)	Defines how the activity assessment was performed: based on geomorphologic evidence only or with additional kinematic data.	1. Kinematic 2. Geomorphologic	RoGI guidelines, Chap. 3 (Sect. 3.4) RoGI guidelines, Chap. 5 (Sect. 5.3)

Table A1. Continued.

Attribute	Description	Values	RGIK guidelines
Acti.Cl. (O)	Activity class assigned to the rock glacier, defined as the efficiency of sediment conveyance (expressed by the surface movement) at the time of observation. See related documentation for further information. Already pre-filled if "Kin.Att." is filled. It is also possible to change the value manually from the drop-down list in the case of low reliability of the kinematic attribute, e.g. due to an unclear pattern in InSAR, unideal slope orientation (N/S) compared to InSAR LOS measurements, or small MAs not covering the entire landform. In such cases, "Kin.Att." may still be documented but assessed as not representative of the real activity of the rock glacier (based on geomorphologic evidence). "Active": rock glacier moving down the slope over most of its surface. "Active uncertain": the rock glacier unit is not in a relict state, but there is not sufficient data or geomorphological evidence to distinguish between an active and transitional state. "Transitional": rock glacier with slow movement only detectable by measurements or movement restricted to areas of non-dominant extent. "Relict uncertain": the rock glacier unit is not in an active state, but there is not sufficient data or geomorphological evidence to distinguish between a transitional and relict state. "Relict": rock glacier with neither geomorphological evidence nor detection of current movement associated with permafrost creep. "Uncertain": the data quality is insufficient to determine an activity status.	1. Active 2. Active uncertain 3. Transitional 4. Relict uncertain 5. Relict 6. Uncertain	RoGI guidelines, Chap. 3 (Sect. 3.4) RoGI guidelines, Chap. 5 (Sect. 5.3) RoGI guidelines, Chap. 6 (Sect. 6.1–6.3) https://doi.org/10.51363/unifr.srr.2023.002
Kin.Att. (O)	Kinematic attribute (KA) assigned to the rock glacier. The kinematic attribute must be representative of the multi-annual movement rate of the rock glacier unit at the time of an inventory. Only if "Acti.Ass." is "Kinematic". The default category is 0, "undefined". The rock glacier unit remains in this category when no (reliable) kinematic information is available, the kinematic information is derived from a single-point survey which cannot be related to any MA, the rock glacier unit is mainly characterised by an identified MA of undefined or unreliable velocity, or the kinematic information is too heterogeneous. See related documentation on the recommendations to document the KA based on a MA layer.	0. Undefined 1. $< \mathrm{cm\,yr^{-1}}$ 2. $\mathrm{cm\,yr^{-1}}$ 3. $\mathrm{cm\,yr^{-1}}$ to $\mathrm{dm\,yr^{-1}}$ 4. $\mathrm{dm\,yr^{-1}}$ 5. $\mathrm{dm\,yr^{-1}}$ to $\mathrm{m\,yr^{-1}}$ 6. $\mathrm{m\,yr^{-1}}$ 7. $> \mathrm{m\,yr^{-1}}$	RoGI guidelines, Chap. 6 (Sect. 6.1–6.3) https://doi.org/10.51363/unifr.srr.2023.002
TypeOfData (O)	Type of data used for kinematic assessment. Use "Kin.Comment" if you want to add more details about the type of date used (e.g. InSAR or SAR offset tracking for "radar"). Only if "Acti.Ass." is "Kinematic". "Other" can be used if there is a combination of methods (add comments in "Kin.Comment").	Optical Radar Lidar Geodetic Other	RoGI guidelines, Chap. 6 (Sect. 6.1–6.3) https://doi.org/10.51363/unifr.srr.2023.002
Kin.Period (O)	Period of the data used to assign the KA (e.g. 2018–2020). Only if "Acti.Ass." is "Kinematic".	yyyy–yyyy	RoGI guidelines, Chap. 6 (Sect. 6.1–6.3) https://doi.org/10.51363/unifr.srr.2023.002

Table A1. Continued.

Attribute	Description	Values	RGIK guidelines
Destabili. (O)	Describes if the rock glacier unit is (ongoing) or has been (completed) destabilised. Destabilisation refers to rock glaciers with obvious signals of abnormally large displacements, often associated with the opening of large transversal cracks and/or scarps. "Yes, ongoing": geomorphological evidence and/or kinematic data signal to an ongoing phase of destabilisation. "Yes, completed": geomorphological evidence and/or kinematic data confirm a completed destabilisation phase.	0. No 1. Yes, ongoing 2. Yes, completed 3. Uncertain	RoGI guidelines, Chap. 3 (Sect. 3.5) RoGI guidelines, Chap. 5 (Sect. 5.3) https://doi.org/10.51363/unifr.srr.2023.002
Kin.Comment (O)	Comment regarding kinematic information, data type and quality, spatial representativeness, etc. It allows for documenting uncertainties, especially when the reliability is low or medium.	Text	
Rel.Kin. (O)	Reliability of the assignment of the KA based on a qualitative assessment of the data quality and spatial heterogeneity. Only if "Acti.Ass." is "Kinematic" The attribute accounts for the reliability of MAs covering the rock glacier, the spatial representativeness of the kinematic information (fraction of the rock glacier that is covered by MAs), and the heterogeneity of the available kinematic information (number of overlapping MAs with potentially different velocity classes). "Low": KA assessment is affected by several of the above listed limitations. "Medium": KA assessment is affected by one of the above listed limitations. "High": no limitation is significantly impacting the KA assessment.	0. Low 1. Medium 2. High	RoGI guidelines, Chap. 6 (Sect. 6.1–6.3) https://doi.org/10.51363/unifr.srr.2023.002
Country (O)	Country code of the RoGI area.	RO: Romania CH: Switzerland NO: Norway (T: Troms, F: Finnmark, N: Nordenskiöld Land) FR: France IT: Italy GL: Greenland KA: Kazakhstan US: USA AR: Argentina NZ: Aotearoa New Zealand	See Table 1 and Sect. 3.3 (naming convention).

Appendix B: Attribute table of the moving area (MA) files

Table B1. Attribute table of the moving area (MA) gpkg files (M: mandatory attribute, O: optional attribute). The table only includes essential definitions necessary to understand the overall meaning of the attributes. The detailed recommendations for delineating MA based on InSAR and assigning values to each attribute are documented in RGIK (2023b).

Attribute	Description	Values
Fid (M)	Unique identifier of the polygon.	Automatic filling
MA.ID. (M)	MA + 12 to 15 digits depending on the "lat" and "long" values. Always four digits after the degrees. (e.g. MA34567S123456E means 3,4567° S and 12,3456° E)	Automatic filling
WorkingID (O)	Practical identifier chosen by the operator (e.g. MA_TYR001 and TYR002 for a moving areas inventory in Tyrol).	Text
Ref.PrimaryID (O)	PrimaryID of the related rock glacier unit in the PM attribute table.	Text
Vel.Class (M)	Velocity class documenting the overall movement rate observed in a MA during a considered time frame and according to a specific observation time window. It refers to a multi-annual surface velocity representative of the rock glacier creep rate. Using InSAR, it refers to the velocity observed in the radar line of sight (LOS) using a dataset covering several months and/or years during a specified observation time window ("Time.Obs.").	0. Undefined 1. $< 1\,\mathrm{cm\,yr^{-1}}$ (no movement up to some $\mathrm{mm\,yr^{-1}}$) 2. 1–3 $\mathrm{cm\,yr^{-1}}$ (some $\mathrm{cm\,yr^{-1}}$) 3. 3–10 $\mathrm{cm\,yr^{-1}}$ 4. 10–30 $\mathrm{cm\,yr^{-1}}$ (some $\mathrm{dm\,yr^{-1}}$) 5. 30–100 $\mathrm{cm\,yr^{-1}}$ 6. $> 100\,\mathrm{cm\,yr^{-1}}$ ($\mathrm{m\,yr^{-1}}$ and higher)
Time.Obs. (O)	Sensor type used to perform the characterisation is documented here – observation time window (period during which the detection and characterisation is computed/measured, i.e. which months/seasons) and temporal frame (total duration during which the periodic measurements/computations are repeated and aggregated for defining the moving area, i.e. which year(s)).	Text containing SENSOR(s) OBSERVATION-TIME-WINDOW TEMPORAL-FRAME, e.g. with InSAR data: S1 summer Y1–Y2 (velocity observed from Sentinel-1 with an observation time window in summer each year between year Y1 and year Y2). TerraSAR-X summer Y1, Y2, … (velocity observed from TerraSAR-X with an observation time window in summer at year Y1, year Y2, etc.) Cosmo-SkyMed annual Y1–Y2 (velocity observed from Cosmo-SkyMed with an observation time window of 1 year each year in between year Y1 and year Y2). ALOS 08–10 Y1–Y2 (velocity observed from ALOS with an observation time window between August and October each year between year Y1 and year Y2) S1 summer Y1–Y2 and TerraSAR-X 10 Y3 (velocity observed from Sentinel-1 with an observation time window in summer each year between year Y1 and year Y2 and TerraSAR-X with an observation time window centred in October of the year Y3) Note: the "summer" period must be described in the metadata, and it should be at least 2–3 months.

Table B1. Continued.

Attribute	Description	Values
Rel.MA (O)	Reliability of the detected moving areas. "Low": signal interpretation (velocity estimation) and outline are uncertain, but there is evidence of movement that needs to be considered. "Medium": signal interpretation (velocity estimation) or outline is uncertain. "High": obvious signal and best appropriate configuration (e.g. slope orientation well aligned with the LOS when using InSAR).	0. Low 1. Medium 2. High
Comment (O)	Comments regarding the MA detection and characterisation (e.g. potential limitations affecting the reliability).	Text (250 characters maximum)
Country (O)	Country code of the RoGI area.	RO: Romania CH: Switzerland NO: Norway (T: Troms, F: Finnmark, N: Nordenskiöld Land) FR: France IT: Italy GL: Greenland KA: Kazakhstan US: U.S.A. AR: Argentina NZ: Aotearoa New Zealand See Table 1 and Sect. 3.3 (naming convention).

Appendix C: Attribute table of the geomorphological outline (GO) layers

Table C1. Attribute table of the geomorphological outline (GO) gpkg files (M: mandatory attribute, O: optional attribute). The table only includes essential definitions necessary to understand the overall meaning of the attributes. The last column refers to the sections of the RGIK guidelines documenting detailed recommendations for outlining rock glaciers and assigning values to each attribute. At the time of the exercise, the table referred to the sections of several dedicated documents (RGIK, 2022b, c). The RGIK RoGI guidelines have since been merged into one reference document (RGIK, 2023a). The following table has therefore been updated accordingly.

Attribute	Description	Values	RGIK guidelines
Fid (M)	Unique identifier of the polygon.	Automatic filling	
PrimaryID (M)	Unique identifier of the rock glacier unit in the PM attribute table. The digitised polygon in this table is necessarily associated with the previously created primary marker (point geometry). "PrimaryID" must, therefore, be the same as the associated primary marker.	Automatic filling	RoGI guidelines, Chap. 5 (Sect. 5.2) https://doi.org/10.51363/unifr.srr.2023.002
WorkingID (O)	Practical identifier chosen by the operator (e.g. TYR001 and TYR002 for an inventory in Tyrol).	Text	

Table C1. Continued.

Attribute	Description	Values	RGIK guidelines
Out.Type (M)	Outline type. "Extended": the outline embeds the entire rock glacier up to the rooting zone and includes the external parts (front and lateral margins). "Restricted": the outline embeds the entire rock glacier up to the rooting zone and excludes the external parts (front and lateral margins). "Other": if other criteria are applied (to be documented in the "comment" field).	1. Extended 2. Restricted 3. Other	RoGI guidelines, Chap. 3 (Sect. 3.6) RoGI guidelines, Chap. 5 (Sect. 5.4) https://doi.org/10.51363/unifr.srr.2023.002
Rel.Fr. (O)	Reliability of the front outline digitalisation. Qualitative assessment depending on the data quality and the geomorphology complexity of the landform.	2. High 1. Medium 0. Low	RoGI guidelines, Chap. 5 (Sect. 5.4.1 and 5.4.4) https://doi.org/10.51363/unifr.srr.2023.002
Rel.LeftLM (O)	Reliability of the left lateral margin (i.e. orographic perspective) outline digitalisation. Qualitative assessment depending on the data quality and the geomorphology complexity of the landform.	2. High 1. Medium 0. Low	RoGI guidelines, Chap. 5 (Sect. 5.4.2 and 5.4.4) https://doi.org/10.51363/unifr.srr.2023.002
Rel.RightLM (O)	Reliability of the right lateral margin (i.e. orographic perspective) outline digitalisation. Qualitative assessment depending on the data quality and the geomorphology complexity of the landform.	2. High 1. Medium 0. Low	RoGI guidelines, Chap. 5 (Sect. 5.4.2 and 5.4.4) https://doi.org/10.51363/unifr.srr.2023.002
Rel.Ups.Con. (O)	Reliability of the upslope connection outline digitalisation. Qualitative assessment depending on the data quality and the geomorphology complexity of the landform.	2. High 1. Medium 0. Low	RoGI guidelines, Chap. 5 (Sect. 5.4.3 and 5.4.4) https://doi.org/10.51363/unifr.srr.2023.002
Rel.Index (O)	Outline reliability index summing the values assigned to the reliability attributes "RelFr", "Rel.LeftLM", "Rel.RightLM", and "Rel.Ups.Con.".	Automatic filling From 0 (Low) to 8 (High)	RoGI guidelines, Chap. 5 (Sect. 5.4.4) https://doi.org/10.51363/unifr.srr.2023.002
Comment (O)	Comments regarding the outline, including information regarding the data source(s) used for the delineation and the uncertainties impacting the reliability of the resulting polygon.	Text (250 characters maximum)	
Country (O)	Country code of the RoGI area.	RO: Romania CH: Switzerland NO: Norway (T: Troms, F: Finnmark, N: Nordenskiöld Land) FR: France IT: Italy GL: Greenland KA: Kazakhstan US: USA AR: Argentina NZ: Aotearoa New Zealand	See Table 1 and Sect. 3.3 (naming convention).

Author contributions. The ESA CCI Permafrost project is managed by TS. LiR and CP coordinate the mountain permafrost component of the project. The multi-operator exercise was designed by RD, TE and LiR. The RoGI instructions and GIS generic tool were prepared by TE, RD, CP and LiR. The InSAR datasets were processed by TS and LiR. LiR set the timeline of the exercise, led coordination meetings with the PIs and oversaw the work between the areas. LS assisted the coordination of the PI meetings. The multi-operator work in each area was coordinated by the PIs: FS (area 5-1), TE (area 6-1), LiR (area 7-1, 8-1, 9-1), DC (area 10-1), FB (area 11-1), RC (area 12-1), TB (area 13-1), MD (area 14-1), LuR (area 15-1) and CL (area 16-1). RD performed the work in all the areas and contributed to coordinate key decisions across the teams. The PIs finalised the products for their area. Technical correction and final data package compilation was performed by TE, LiR, LS and RD. LiR led the work on writing and revising the manuscript. Figures and tables were made by TE and LiR. All authors contributed to the final version of the paper.

Competing interests. The contact author has declared that none of the authors has any competing interests.

Disclaimer. Publisher's note: Copernicus Publications remains neutral with regard to jurisdictional claims made in the text, published maps, institutional affiliations, or any other geographical representation in this paper. While Copernicus Publications makes every effort to include appropriate place names, the final responsibility lies with the authors.

Acknowledgement. We acknowledge the effort of the other operators of the RoGI exercise, listed here in alphabetic order: Xavier Bodin, George Brencher, Javiera Carrasco, Daniel Costantini, Thibaut Duvanel, Daniel Falaschi, David Farías-Barahona, Lidia Ferri, Alexander Handwerger, Paula Johns, Nina Jones, Kaytan Kelkar, Alexandru Onaca, Silvia Pasquali, Ivanna Pecker, Razvan Popescu, Benjamin Robson, Cristina San Martin, Nicole Schaffer, Monika Schnitzer, Riccardo Scotti, Zhangyu Sun, David Tonidandel, Julie Wee, Mishelle Wehbe, Lotte Wendt, Ella Wood, and Laura Zalazar. We acknowledge the work of Alina Milceva, who helped revise the outlines and set up the WebGIS tool. We thank Tim Kerr for his open comment, and the two anonymous reviewers for their great referee reports, which provided constructive suggestions to improve the dataset and associated paper.

Financial support. The initiative is funded by the European Space Agency Permafrost Climate Change Initiative (ESA CCI Permafrost, contract 4000123681/18/I-NB). The work of the Rock Glacier Inventories and Kinematics (RGIK) community has been supported by the International Permafrost Association (IPA), GCOS Switzerland, and SwissUniversities.

Review statement. This paper was edited by Chris DeBeer and reviewed by two anonymous referees.

References

Ardelean, A. C., Onaca, A. L., Urdea, P., Serban, R. D., and Sirbu, F.: A first estimate of permafrost distribution from BTS measurements in the Romanian Carpathians (Retezat Mountains), Geomorphologie, 21, 297–312, https://doi.org/10.4000/geomorphologie.11131, 2015.

Azócar, G. F., Brenning, A., and Bodin, X.: Permafrost distribution modelling in the semi-arid Chilean Andes, The Cryosphere, 11, 877–890, https://doi.org/10.5194/tc-11-877-2017, 2017.

Bartsch, A., Strozzi, T., and Nitze, I.: Permafrost monitoring from space, Surv. Geophys., 44, 1579–1613, https://doi.org/10.1007/s10712-023-09770-3, 2023.

Berthling, I., Etzelmüller, B., Eiken, T., and Sollid, J. L.: Rock glaciers on Prins Karls Forland, Svalbard. I: internal structure, flow velocity and morphology, Permafrost Periglac., 9, 135–145, https://doi.org/10.1002/(SICI)1099-1530(199804/06)9:2<135::AID-PPP284>3.0.CO;2-R, 1998.

Bertone, A., Barboux, C., Bodin, X., Bolch, T., Brardinoni, F., Caduff, R., Christiansen, H. H., Darrow, M. M., Delaloye, R., Etzelmüller, B., Humlum, O., Lambiel, C., Lilleøren, K. S., Mair, V., Pellegrinon, G., Rouyet, L., Ruiz, L., and Strozzi, T.: Incorporating InSAR kinematics into rock glacier inventories: insights from 11 regions worldwide, The Cryosphere, 16, 2769–2792, https://doi.org/10.5194/tc-16-2769-2022, 2022.

Bertone, A., Jones, N., Mair, V., Scotti, R., Strozzi, T., and Brardinoni, F.: A climate-driven, altitudinal transition in rock glacier dynamics detected through integration of geomorphological mapping and synthetic aperture radar interferometry (InSAR)-based kinematics, The Cryosphere, 18, 2335–2356, https://doi.org/10.5194/tc-18-2335-2024, 2024.

Blöthe, J. H., Halla, C., Schwalbe, E., Bottegal, E., Trombotto Liaudat, D., and Schrott, L.: Surface velocity fields of active rock glaciers and ice-debris complexes in the Central Andes of Argentina, Earth Surf. Proc. Land., 46, 504–522, https://doi.org/10.1002/esp.5042, 2021.

Bodin, X., Krysiecki, J. M., Schoeneich, P., Le Roux, O., Lorier, L., Echelard, T., Peyron, M., and Walpersdorf, A.: The 2006 collapse of the Bérard rock glacier (Southern French Alps), Permafrost Periglac., 28, 209–223, https://doi.org/10.1002/ppp.1887, 2017.

Boeckli, L., Brenning, A., Gruber, S., and Noetzli, J.: A statistical approach to modelling permafrost distribution in the European Alps or similar mountain ranges, The Cryosphere, 6, 125–140, https://doi.org/10.5194/tc-6-125-2012, 2012.

Bolch, T. and Gorbunov, A. P.: Characteristics and origin of rock glaciers in Northern Tien Shan (Kazakhstan/Kyrgyzstan), Permafrost Periglac., 25, 320–332, https://doi.org/10.1002/ppp.1825, 2014.

Brardinoni, F., Scotti, R., Sailer, R., and Mair, V.: Evaluating sources of uncertainty and variability in rock glacier inventories, Earth Surf. Proc. Land., 44, 2450–2466, https://doi.org/10.1002/esp.4674, 2019.

Brencher, G., Handwerger, A. L., and Munroe, J. S.: InSAR-based characterization of rock glacier movement in the Uinta Mountains, Utah, USA, The Cryosphere, 15, 4823–4844, https://doi.org/10.5194/tc-15-4823-2021, 2021.

Calkin, P. E.: Rock glaciers of central Brooks Range, Alaska, USA, in: Rock glaciers, edited by: Giardino, J. R., Shroder, J. F., and

Vitek, J. D., Allen & Unwin, Boston, 65–82, ISBN 978-0-04-551139-6, 1987.

Cicoira, A., Beutel, J., Faillettaz, J., and Vieli, A.: Water controls the seasonal rhythm of rock glacier flow, Earth Planet. Sc. Lett., 528, 115844, https://doi.org/10.1016/j.epsl.2019.115844, 2019.

Delaloye, R., Perruchoud, E., Avian, M., Kaufmann, V., Bodin, X., Hausmann, H., Ikeda, A., Kääb, A., Kellerer-Pirklbauer, A., Krainer, K., Lambiel, C., Mihajlovic, D., Staub, B., Roer, I., and Thibert, E.: Recent interannual variations of rock glacier creep in the European Alps, in: 9th International Conference on Permafrost, 29 June–3 July 2008, Fairbanks, Alaska, 343–348, https://doi.org/10.5167/uzh-7031, 2008.

Delaloye, R., Lambiel, C., and Gärtner-Roer, I.: Overview of rock glacier kinematics research in the Swiss Alps, Geogr. Helv., 65, 135–145, https://doi.org/10.5194/gh-65-135-2010, 2010.

Delaloye, R., Morard, S., Barboux, C., Abbet, D., Gruber, V., Riedo, M., and Gachet, S.: Rapidly moving rock glaciers in Mattertal. Mattertal – ein Tal in Bewegung, in: Mattertal – ein Tal in Bewegung, Publikation zur Jahrestagung der Schweizerischen Geomorphologischen Gesellschaft, 29 Juni–1. Juli 2011, St. Niklaus, Birmensdorf, Eidg. Forschungsanstalt WSL, 21–31, ISBN 978-3-905621-53-2, 2013.

Delaloye, R., Barboux, C., Bodin, X., Brenning, A., Hartl, L., Hu, Y., Ikeda, A., Kaufmann, V., Kellerer-Pirklbauer, A., Lambiel, C., and Liu, L.: Rock glacier inventories and kinematics: A new IPA Action Group, in: vol. 23, Proc. EUCOP5 – 5th European Conference of Permafrost, Chamonix, France, 392–393, https://www.unifr.ch/geo/geomorphology/en/assets/public/files/IPA/185466_EUCOP2018_extended_abstract_Delaloye_et_al.pdf (last access: 15 August 2025), 2018.

Ellis, J. M. and Calkin, P. E.: Nature and distribution of glaciers, neoglacial moraines, and rock glaciers, east-central Brooks Range, Alaska, Arct. Alp. Res., 11, 403–420, https://doi.org/10.1080/00040851.1979.12004149, 1979.

Erharter, G. H., Wagner, T., Winkler, G., and Marcher, T.: Machine learning–an approach for consistent rock glacier mapping and inventorying–example of Austria, Applied Computing and Geosciences, 16, 100093, https://doi.org/10.1016/j.acags.2022.100093, 2022.

Eriksen, H. Ø., Rouyet, L., Lauknes, T. R., Berthling, I., Isaksen, K., Hindberg, H., Larsen, Y., and Corner, G. D.: Recent acceleration of a rock glacier complex, Adjet, Norway, documented by 62 years of remote sensing observations, Geophys. Res. Lett., 45, 8314–8323, https://doi.org/10.1029/2018GL077605, 2018.

Etzelmüller, B., Patton, H., Schomacker, A., Czekirda, J., Girod, L., Hubbard, A., Lilleøren, K. L., and Westermann, S.: Icelandic permafrost dynamics since the Last Glacial Maximum–model results and geomorphological implications, Quaternary Sci. Rev., 233, 106236, https://doi.org/10.1016/j.quascirev.2020.106236, 2020.

Farbrot, H., Isaksen, K., Eiken, T., Kääb, A., and Sollid, J. L.: Composition and internal structures of a rock glacier on the strandflat of western Spitsbergen, Svalbard, Norsk Geogr. Tidsskr., 59, 139–148, https://doi.org/10.1080/00291950510020619, 2005.

French, H. M.: The Periglacial Environment, in: 3rd Edn., John Wiley & Sons, https://doi.org/10.1002/9781118684931, 2007.

Gisnås, K., Etzelmüller, B., Lussana, C., Hjort, J., Sannel, A. B. K., Isaksen, K., Westermann, S., Kuhry, P., Christiansen, H. H., Frampton, A., and Åkerman, J.: Permafrost map for Norway, Sweden and Finland, Permafrost Periglac., 28, 359–378, https://doi.org/10.1002/ppp.1922, 2017.

Gorbunov, A. and Titkov, S.: Kamennye Gletchery Gor Srednej Azii: (Rock glaciers of the Central Asian mountains), Akademia Nauk SSSR, Irkutsk, 1989.

Gorbunov, A. P., Titkov, S. N., and Polyakov, V.: Dynamics of the rock glaciers of the Northern Tien Shan and the Djungar Alatau, Kazakhstan, Permafrost Periglac., 3, 29–39, https://doi.org/10.1002/ppp.3430030105, 1992.

Hartl, L., Zieher, T., Bremer, M., Stocker-Waldhuber, M., Zahs, V., Höfle, B., Klug, C., and Cicoira, A.: Multi-sensor monitoring and data integration reveal cyclical destabilization of the Äußeres Hochebenkar rock glacier, Earth Surf. Dynam., 11, 117–147, https://doi.org/10.5194/esurf-11-117-2023, 2023.

Hassan, J., Chen, X., Muhammad, S., and Bazai, N. A.: Rock glacier inventory, permafrost probability distribution modeling and associated hazards in the Hunza River Basin, Western Karakoram, Pakistan, Sci. Total Environ., 782, 146833, https://doi.org/10.1016/j.scitotenv.2021.146833, 2021.

Hu, Y., Liu, L., Huang, L., Zhao, L., Wu, T., Wang, X., and Cai, J.: Mapping and characterizing rock glaciers in the arid Western Kunlun Mountains supported by InSAR and deep learning, J. Geophys. Res.-Earth, 128, e2023JF007206, https://doi.org/10.1029/2023JF007206, 2023.

Hu, Y., Arenson, L. U., Barboux, C., Bodin, X., Cicoira, A., Delaloye, R., Gärtner-Roer, I., Kääb, A., Kellerer-Priklbauer, A., Lambiel, C., Liu, L., Pellet, C., Rouyet. L., Schoeneich, P., Seier, G., and Strozzi, T.: Rock glacier velocity: An Essential Climate Variable Quantity for Permafrost, Rev. Geophys., 63, e2024RG000847, https://doi.org/10.1029/2024RG000847, 2025.

Humlum, O.: Rock glacier types on Disko, Central West Greenland, Geogr. Tidsskr., 82, 59–66, https://doi.org/10.1080/00167223.1982.10649152, 1982.

Humlum, O.: Origin of rock glaciers: Observations from Mellemfjord, Disko Island, Central West Greenland, Permafrost Periglac., 7, 361–380, https://doi.org/10.1002/(SICI)1099-1530(199610)7:4<361::AID-PPP227>3.0.CO;2-4, 1996.

Ikeda, A. and Matsuoka, N.: Degradation of talus-derived rock glaciers in the Upper Engadin, Swiss Alps, Permafrost Periglac., 13, 145–161, https://doi.org/10.1002/ppp.413, 2002.

Ikeda, A., Matsuoka, N., and Kääb, A.: Fast deformation of perennially frozen debris in a warm rock glacier in the Swiss Alps: An effect of liquid water, J. Geophys. Res.-Earth, 113, F01021, https://doi.org/10.1029/2007JF000859, 2008.

Isaksen, K., Ødegård, R. S., Eiken, T., and Sollid, J. L.: Composition, flow and development of two tongue-shaped rock glaciers in the permafrost of Svalbard, Permafrost Periglac., 11, 241–257, https://doi.org/10.1002/1099-1530(200007/09)11:3<241::AID-PPP358>3.0.CO;2-A, 2000.

Jones, D. B., Harrison, S., Anderson, K., Selley, H. L., Wood, J. L., and Betts, R. A.: The distribution and hydrological significance of rock glaciers in the Nepalese Himalaya, Global Planet. Change, 160, 123–142, https://doi.org/10.1016/j.gloplacha.2017.11.005, 2018.

Kääb, A., Frauenfelder, R., and Roer, I.: On the response of rockglacier creep to surface temperature increase, Global Planet. Change, 56, 172–187, https://doi.org/10.1016/j.gloplacha.2006.07.005, 2007.

Kääb, A., Strozzi, T., Bolch, T., Caduff, R., Trefall, H., Stoffel, M., and Kokarev, A.: Inventory and changes of rock glacier creep speeds in Ile Alatau and Kungöy Ala-Too, northern Tien Shan, since the 1950s, The Cryosphere, 15, 927–949, https://doi.org/10.5194/tc-15-927-2021, 2021.

Karjalainen, O., Luoto, M., Aalto, J., Etzelmüller, B., Grosse, G., Jones, B. M., Lilleøren, K. S., and Hjort, J.: High potential for loss of permafrost landforms in a changing climate, Environ. Res. Lett., 15, 104065, https://doi.org/10.1088/1748-9326/abafd5, 2020.

Kellerer-Pirklbauer, A., Bodin, X., Delaloye, R., Lambiel, C., Gärtner-Roer, I., Bonnefoy-Demongeot, M., Carturan, L., Damm, B., Eulenstein, J., Fischer, A., Hartl, L., Ikeda, A., Kaufmann, V., Krainer, K., Matsuoka, N., Morra Di Cella, U., Noetzli, J., Seppi, R., Scapozza, C., Schoeneich, P., Stocker-Waldhuber, M., Thibert, E., and Zumiani, M.: Acceleration and interannual variability of creep rates in mountain permafrost landforms (rock glacier velocities) in the European Alps in 1995–2022, Environ. Res. Lett., 19, 034022, https://doi.org/10.1088/1748-9326/ad25a4, 2024.

Kenner, R., Pruessner, L., Beutel, J., Limpach, P., and Phillips, M.: How rock glacier hydrology, deformation velocities and ground temperatures interact: Examples from the Swiss Alps, Permafrost Periglac., 31, 3–14, https://doi.org/10.1002/ppp.2023, 2020.

Lambiel, C., Strozzi, T., Paillex, N., Vivero, S., and Jones, N.: Inventory and kinematics of active and transitional rock glaciers in the Southern Alps of New Zealand from Sentinel-1 InSAR, Arct. Antarct. Alp. Res., 55, 2183999, https://doi.org/10.1080/15230430.2023.2183999, 2023.

Lilleøren, K. S. and Etzelmüller, B.: A regional inventory of rock glaciers and ice-cored moraines in Norway, Geogr. Ann. A, 93, 175–191, https://doi.org/10.1111/j.1468-0459.2011.00430.x, 2011.

Lilleøren, K. S., Etzelmüller, B., Schuler, T. V., Gisnås, K., and Humlum, O.: The relative age of mountain permafrost – estimation of Holocene permafrost limits in Norway, Global Planet. Change, 92, 209–223, https://doi.org/10.1016/j.gloplacha.2012.05.016, 2012.

Lilleøren, K. S., Etzelmüller, B., Rouyet, L., Eiken, T., Slinde, G., and Hilbich, C.: Transitional rock glaciers at sea level in northern Norway, Earth Surf. Dynam., 10, 975–996, https://doi.org/10.5194/esurf-10-975-2022, 2022.

Liu, L., Millar, C. I., Westfall, R. D., and Zebker, H. A.: Surface motion of active rock glaciers in the Sierra Nevada, California, USA: inventory and a case study using InSAR, The Cryosphere, 7, 1109–1119, https://doi.org/10.5194/tc-7-1109-2013, 2013.

Lugon, R. and Delaloye, R.: Modelling alpine permafrost distribution, Val de Réchy, Valais Alps (Switzerland), Norsk Geogr. Tidsskr., 55, 224–229, https://doi.org/10.1080/00291950152746568, 2001.

Ma, Q. and Oguchi, T.: Rock Glacier Inventory of the Southwestern Pamirs Supported by InSAR Kinematics, Remote Sens.-Basel, 16, 1185, https://doi.org/10.3390/rs16071185, 2024.

Mahanta, K. K., Pradhan, I. P., Gupta, S. K., and Shukla, D. P.: Assessing Machine Learning and Statistical Methods for Rock Glacier-Based Permafrost Distribution in Northern Kargil Region, Permafrost Periglac., 35, 262–277, https://doi.org/10.1002/ppp.2240, 2024.

Manchado, A. M.-T., Allen, S., Cicoira, A., Wiesmann, S., Haller, R., and Stoffel, M.: 100 years of monitoring in the Swiss National Park reveals overall decreasing rock glacier velocities, Communications Earth & Environment, 5, 138, https://doi.org/10.1038/s43247-024-01302-0, 2024.

Marcer, M., Bodin, X., Brenning, A., Schoeneich, P., Charvet, R., and Gottardi, F.: Permafrost favorability index: spatial modeling in the French Alps using a rock glacier inventory, Front. Earth Sci., 5, 105, https://doi.org/10.3389/feart.2017.00105, 2017.

Marcer, M., Serrano, C., Brenning, A., Bodin, X., Goetz, J., and Schoeneich, P.: Evaluating the destabilization susceptibility of active rock glaciers in the French Alps, The Cryosphere, 13, 141–155, https://doi.org/10.5194/tc-13-141-2019, 2019.

Marcer, M., Cicoira, A., Cusicanqui, D., Bodin, X., Echelard, T., Obregon, R., and Schoeneich, P.: Rock glaciers throughout the French Alps accelerated and destabilised since 1990 as air temperatures increased, Communications Earth & Environment, 2, 81, https://doi.org/10.1038/s43247-021-00150-6, 2021.

Marchenko, S. S.: A model of permafrost formation and occurrences in the intracontinental mountains, Norsk Geogr. Tidsskr., 55, 230–234, https://doi.org/10.1080/00291950152746577, 2001.

Marthaler, M., Sartori, M., and Escher, A.: Feuille 1307 Vissoie, Atlas géol. Suisse 1 : 25 000, Carte 122 (Sheet 1307 Vissoie, Swiss Geological Atlas 1 : 25 000, Map 122), ISBN 978-3-302-40018-1, 2008.

Necsoiu, M., Onaca, A., Wigginton, S., and Urdea, P.: Rock glacier dynamics in Southern Carpathian Mountains from high-resolution optical and multi-temporal SAR satellite imagery, Remote Sens. Environ., 177, 21–36, https://doi.org/10.1016/j.rse.2016.02.025, 2016.

Onaca, A., Ardelean, A. C., Urdea, P., Ardelean, F., and Sirbu, F.: Detection of mountain permafrost by combining conventional geophysical methods and thermal monitoring in the Retezat Mountains, Romania, Cold Reg. Sci. Technol., 119, 111–123, https://doi.org/10.1016/j.coldregions.2015.08.001, 2015.

PERMOS: PERMOS Database, Swiss Permafrost Monitoring Network, Davos and Fribourg, Switzerland, https://doi.org/10.13093/permos-2024-01, 2024.

Perruchoud, E. and Delaloye, R.: Short-term changes in surface velocities on the Becs-de-Bosson rock glacier (western Swiss Alps), in: Proceedings HMRSC-IX, Graz, 14–15 September 2006, Grazer Schriften der Geographie und Raumforschung, 43, 131–136, 2007.

Popescu, R., Filhol, S., Etzelmüller, B., Vasile, M., Pleşoianu, A., Vîrghileanu, M., Onaca, A., Şandric, I., Săvulescu, I., Cruceru, N., Vespremeanu-Stroe, A., Westermann, S., Sîrbu, F., Mihai, B., Nedelea, A., and Gascoin, S.: Permafrost Distribution in the Southern Carpathians, Romania, Derived From Machine Learning Modeling, Permafrost Periglac., 35, 243–261, https://doi.org/10.1002/ppp.2232, 2024.

Rangecroft, S., Harrison, S., and Anderson, K.: Rock glaciers as water stores in the Bolivian Andes: an assessment of their hydrological importance, Arct. Antarct. Alp. Res., 47, 89–98, https://doi.org/10.1657/AAAR0014-029, 2015.

Reinosch, E., Gerke, M., Riedel, B., Schwalb, A., Ye, Q., and Buckel, J.: Rock glacier inventory of the western Nyainqêntanglha Range, Tibetan Plateau, supported by InSAR time series

and automated classification, Permafrost Periglac., 32, 657–672, https://doi.org/10.1002/ppp.2117, 2021.

RGIK: Optional kinematic attribute in standardized rock glacier inventories (version 3.0.1, 22 July 2022), IPA Action Group Rock Glacier Inventories and Kinematics (RGIK), 8 pp., https://www.unifr.ch/geo/geomorphology/en/research/ipa-action-group-rock-glacier/ (last access: 15 August 2025), 2022a.

RGIK: Towards standard guidelines for inventorying rock glaciers: baseline concepts (version 4.2.2, 31 March 2022), IPA Action Group Rock Glacier Inventories and Kinematics (RGIK), 13 pp., https://www.unifr.ch/geo/geomorphology/en/research/ipa-action-group-rock-glacier/ (last access: 15 August 2025), 2022b.

RGIK: Towards standard guidelines for inventorying rock glaciers: practical concepts (version 2.0, 11 April 2022), IPA Action Group Rock Glacier Inventories and Kinematics (RGIK), 10 pp., https://www.unifr.ch/geo/geomorphology/en/research/ipa-action-group-rock-glacier/ (last access: 15 August 2025), 2022c.

RGIK: Guidelines for inventorying rock glaciers: baseline and practical concepts (version 1.0, 28 December 2023), IPA Action Group Rock Glacier Inventories and Kinematics, 25 pp., https://doi.org/10.51363/unifr.srr.2023.002, 2023a.

RGIK: InSAR-based kinematic attribute in rock glacier inventories. Practical InSAR Guidelines (version 4.0., 31 May 2023), IPA Action Group Rock Glacier Inventories and Kinematics (RGIK), 33 pp., https://www.rgik.org (last access: 15 August 2025), 2023b.

RGIK: Rock Glacier Velocity as an associated parameter of ECV Permafrost: baseline concepts (version 3.2, 22 May 2023), IPA Action Group Rock Glacier Inventories and Kinematics (RGIK), 13 pp., https://www.rgik.org (last access: 15 August 2025), 2023c.

RGIK: Rock Glacier Inventories and Kinematics (RGIK) Guidelines and QGIS tools, https://www.rgik.org/resources/ (last access: 15 August 2025), 2025.

Robson, B. A., Bolch, T., MacDonell, S., Hölbling, D., Rastner, P., and Schaffer, N.: Automated detection of rock glaciers using deep learning and object-based image analysis, Remote Sens. Environ., 250, 112033, https://doi.org/10.1016/j.rse.2020.112033, 2020.

Rouyet, L., Lilleøren, K. S., Böhme, M., Vick, L. M., Delaloye, R., Etzelmüller, B., Lauknes, T. R., Larsen, Y., and Blikra, L. H.: Regional morpho-kinematic inventory of slope movements in northern Norway, Front. Earth Sci., 9, 681088, https://doi.org/10.3389/feart.2021.681088, 2021.

Rouyet, L., Bolch, T., Brardinoni, F., Caduff, R., Cusicanqui, D., Darrow, M., Delaloye, R., Echelard, T., Lambiel, C., Pellet, C., Ruiz, L., Schmid, L., Sirbu, F., and Strozzi, T.: Rock Glacier Inventories (RoGI) in 12 areas worldwide using a multi-operator consensus-based procedure, Zenodo [data set], https://doi.org/10.5281/zenodo.14501398, 2025.

Sattler, K., Anderson, B., Mackintosh, A., Norton, K., and de Róiste, M.: Estimating permafrost distribution in the maritime southern alps, New Zealand, based on climatic conditions at rock glacier sites, Front. Earth Sci., 4, 1–17, https://doi.org/10.3389/feart.2016.00004, 2016.

Schmid, M.-O., Baral, P., Gruber, S., Shahi, S., Shrestha, T., Stumm, D., and Wester, P.: Assessment of permafrost distribution maps in the Hindu Kush Himalayan region using rock glaciers mapped in Google Earth, The Cryosphere, 9, 2089–2099, https://doi.org/10.5194/tc-9-2089-2015, 2015.

Schoeneich, P., Bodin, X., Echelard, T., Kaufmann, V., Kellerer-Pirklbauer, A., Krysiecki, J.-M., and Lieb, G. K.: Velocity Changes of Rock Glaciers and Induced Hazards, in: Engineering Geology for Society and Territory – Vol. 1, edited by: Lollino, G., Manconi, A., Clague, J., Shan, W., and Chiarle, M., Springer, Cham, https://doi.org/10.1007/978-3-319-09300-0_42, 2015.

Scotti, R., Crosta, G. B., and Villa, A.: Destabilisation of Creeping Permafrost: The Plator Rock Glacier Case Study (Central Italian Alps), Permafrost Periglac., 28, 224–236, https://doi.org/10.1002/ppp.1917, 2017.

Scotti, R., Mair, V., Costantini, D., and Brardinoni, F.: A high-resolution rock glacier inventory of South Tyrol: Evaluating lithologic, topographic, and climatic effects, in: 12th International Conference on Permafrost, edited by: Beddoe, R. A. and Karunaratne, K. C., 16–20 June 2024, International Permafrost Association, Whitehorse, Canada, 382–389, https://doi.org/10.52381/ICOP2024.176.1, 2024.

Staub, B., Lambiel, C., and Delaloye, R.: Rock glacier creep as a thermally-driven phenomenon: A decade of inter-annual observations from the Swiss Alps, in: 11th International Conference on Permafrost, 20–24 June 2016, Potsdam, Germany, Bibliothek Wissenschaftspark Albert Einstein, 96–97, 2016.

Streletskiy, D., Biskaborn, B., Smith, S. L., Noetzli, J., Viera, G., and Schoeneich, P.: Strategy and Implementation Plan 2016–2020 for the Global Terrestrial Network for Permafrost (GTN-P), https://library.arcticportal.org/id/eprint/1938 (last access: 15 August 2025), 2017.

Streletskiy, D., Noetzli, J., Smith, S. L., Vieira, G., Schoeneich, P., Hrbacek, F., and Irrgang A. M.: Strategy and Implementation Plan 2021–2024 for the Global Terrestrial Network for Permafrost (GTN-P), https://doi.org/10.5281/zenodo.6075467, 2021.

Sun, Z., Hu, Y., Racoviteanu, A., Liu, L., Harrison, S., Wang, X., Cai, J., Guo, X., He, Y., and Yuan, H.: TPRoGI: a comprehensive rock glacier inventory for the Tibetan Plateau using deep learning, Earth Syst. Sci. Data, 16, 5703–5721, https://doi.org/10.5194/essd-16-5703-2024, 2024.

Tenthorey, G.: Perennial névés and the hydrology of rock glaciers, Permafrost Periglac., 3, 247–252, https://doi.org/10.1002/ppp.3430030313, 1992.

Titkov, S. N.: Rock Glaciers and glaciation of the Central Asian Mountains, in: vol. 1, Proceedings of the 5th International Permafrost Conference, Trondheim, 2–5 August 1988, 259–262, ISBN 978-82-519-0863-4, 1988.

Trofaier, A. M., Westermann, S., and Bartsch, A.: Progress in space-borne studies of permafrost for climate science: Towards a multi-ECV approach, Remote Sens. Environ., 203, 55–70, https://doi.org/10.1016/j.rse.2017.05.021, 2017.

Trombotto-Liaudat, D.: Survey of cryogenic processes, periglacial forms and permafrost conditions in South America, Revista do Instituto Geológico, 21, 33–55, https://doi.org/10.5935/0100-929X.20000004, 2000.

Trombotto-Liaudat, D. and Bottegal, E.: Recent evolution of the active layer in the Morenas Coloradas rock glacier, Central An-

des, Mendoza, Argentina and its relation with kinematics, CIG, https://doi.org/10.18172/cig.3946, 2019.

UNIFR: WebGIS ESA CCI+ Permafrost Project – Rock Glacier Inventories, University of Fribourg (UNIFR), https://bigweb.unifr.ch/Science/Geosciences/Geomorphology/Pub/Website/CCI/CCI_qgis2web_2025_04 (last access: 15 August 2025), 2025.

Way, R. G., Wang, Y., Bevington, A. R., Bonnaventure, P. P., Burton, J. R., Davis, R., Garibaldi, M. C., Lapalme, C. M., Tutton, R., and Wehbe, M. A.: Consensus-Based Rock Glacier Inventorying in the Torngat Mountains, Northern Labrador, in: Proc. Regional Conference on Permafrost 2021 and the 19th International Conference on Cold Regions Engineering, American Society of Civil Engineers, Reston, VA, 24–29 October 2021, 130–141, ISBN 978-1-7138-3849-4, 2021.

WMO: The 2022 GCOS ECVs Requirements, GCOS – 245, World Meteorological Organization (WMO), https://library.wmo.int/idurl/4/58111 (last access: 15 August 2025), 2022.

Zalazar, L., Ferri, L., Castro, M., Gargantini, H., Gimenez, M., Pitte, P., Ruiz, L., Masiokas, M., Costa, G., and Villalba, R.: Spatial distribution and characteristics of Andean ice masses in Argentina: results from the first National Glacier Inventory, J. Glaciol., 66, 938–949, https://doi.org/10.1017/jog.2020.55, 2020.